Cross-kingdom affairs: Can microRNAs of host plants regulate genes of their insect herbivores?

विद्या वाचस्पति की
उपाधि की अपेक्षाओं की आंशिक पूर्ति में प्रस्तुत शोध प्रबंध

A thesis submitted in partial fulfillment of the requirements of the degree of Doctor of Philosophy

द्वारा / By
ऋत्विक बर्दापूरकर / Rutwik Bardapurkar

पंजीकरण सं. / Registration No.: 20152009

शोध प्रबंध पर्यवेक्षक / Thesis Supervisor: Dr. Sagar Pandit

भारतीय विज्ञान शिक्षा एवं अनुसंधान संस्थान पुणे
INDIAN INSTITUTE OF SCIENCE EDUCATION AND RESEARCH PUNE

2024

Dedication

I dedicate this thesis to Aai, Baba, and my mentors.

Declaration

I declare that this written submission represents my ideas in my own words and where others' ideas have been included, I have adequately cited and referenced the original sources. I also declare that I have adhered to all principles of academic honesty and integrity and have not misrepresented or fabricated or falsified any idea/data/fact/source in my submission. I understand that violation of the above will be cause for disciplinary action by the Institute and can also evoke penal action from the sources which have thus not been properly cited or from whom proper permission has not been taken when needed.

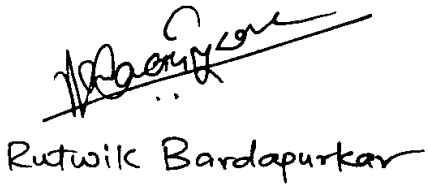

Rutwik Bardapurkar
20152009

Date: 20th May, 2024

Certificate

Certified that the work incorporated in the thesis entitled "Cross-kingdom affairs: Can microRNAs of host plants regulate genes of their insect herbivores?" submitted by Mr. Rutwik Bardapurkar was carried out by the candidate, under my supervision. The work presented here or any part of it has not been included in any other thesis submitted previously for the award of any degree or diploma from any other university or institution.

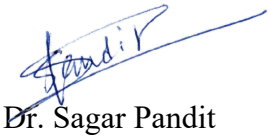

Dr. Sagar Pandit

Date: 20th May, 2024

Acknowledgments

I extend my deepest gratitude to everyone who has played pivotal roles in my academic journey. Firstly, Dr. Sagar Pandit, my Ph.D. supervisor, whose unwavering support, guidance, and belief in my abilities have been invaluable. His knowledge and expertise, especially in scientific writing and public speaking, have significantly contributed to my development. Under his mentorship, I have developed grit, discipline, focus, and a profound interest in how to do good science. Beyond academics, Dr. Pandit has also nurtured my life skills and consistently encouraged me to become an independent scientific professional. I am indebted to him for training me to gain clarity of thought in every step, be it experimenting, presenting, or writing. I sincerely thank him for being one of the strongest supports in my life. I also appreciate the contributions of Prof. Anjan Banerjee, Dr. Narendra Kadoo, and Dr. Krishanpal Karmodiya, members of the Research Advisory Committee, for their insightful evaluations of my progress. My heartfelt thanks go to IISER Pune for providing a multidisciplinary research platform, world-class facilities, and an integrated Ph.D. fellowship. The unwavering support of the technical staff at IISER Pune has been instrumental in the completion of my thesis. In the ABCE Lab at IISER Pune, I express my gratitude to Dr. Ashish B. Deshpande, Ms. Bhumika Upadhyay, Mr. Surhud Sant, Mr. Maruf Shaikh, Mr. Mahendra Pawar, Ms. Prashasti Pandey, Mr. Dennis Metze, Mr. Sujay Paranjape, Ms. Prajakta Ingale, Ms. Drashti Borad, Mr. Umesh KP, Ms. Namithashree M, Mr. Kankan Datta, Ms. Priyanka, Mr. Showkat Nissar, Mr. Tushar Gavali, Mr. Viraj Jangam, and Ms. Sonam Shinde for being such great lab members, for the energy that they brought to the lab and their forever support and aid. I want to thank the army of people who worked with me, including Mr. Dheerendra Singh, Mr. Surhud Sant, Ms. Bhawana, Ms. Roshni Das, Mr. Mihir Joshi, Mr. Sahil Pawar, Ms. Tharangini, Ms. Sowmya, Ms. Prashasti Pandey, Ms. Kaushiki Kandalgaonkar, Ms. Bhavya Sehara, Ms. Khushi Choksi, Ms. Rashi Gupta, Ms. Rutuja Ugale, Mr. Subramanya Gond, Ms. Tiana Pinto, and many more. I also appreciate the exceptional aid of Mr. Ganesh Pawar, our field assistant. His dedication and selfless attitude were the strongest force bringing the work in the lab to fruition. I also thank Mr. Nitish Lahigude for maintaining experimental facilities. Being with the three pillars, Dr. Rituparna Ghosh, Dr. Manish Kumar, and Dr. Gauri Binayak was one of the greatest pleasures of this lab. They were with me through all the ups and downs, and I am most grateful to them. Their support, scientific insights, and critical comments and suggestions have shaped me as a better scientist and a human being. I want to thank my parents, Mr. Vinay Bardapurkar and Mrs. Anjali Bardapurkar, and my grandparents, Mr. Shriram Bardapurkar and the late Mrs. Rajani Bardapurkar, for supporting me in this venture and giving me complete freedom to choose my career path. Their selfless support and sacrifice are why I could complete this body of work. I owe my gratitude to them. The positivity and encouragement of all my teachers throughout my academic journey are also deeply appreciated. Being part of the ABCE Lab at IISER Pune has been a rewarding experience, and I am thankful to everyone who has contributed to my growth and success.

Contents

List of figures

List of tables

List of acronyms

C: Artificial diet

pre-C: pre-let-7 control mixed in C

mature-C: let-7 mature miRNA duplex mixed in C

CP-pre: miRNA pre-forms of the common miRNA pairs from the miRNA-target *in silico* analysis

nCP-pre: miRNA pre-forms of the common miRNA pairs from the miRNAs not in the analysis

Dme-pre: *D. melanogaster* pre-miRNAs

Pxy-pre: *P. xylostella* pre-miRNAs

Dme-AGO-2-md: Dme: *D. melanogaster* miRNA duplexes binding to AGO-2

Pxy-md: *P. xylostella* miRNA duplexes binding to AGO-2

CP-md: miRNA duplexes of the common miRNA pairs from the miRNA-target *in silico* analysis

nCP-md: miRNA duplexes of the common miRNA pairs from the miRNAs not in the analysis

Hb: Herbivory

W+OS: Wounding + oral secretion complemented

W+W: Wounding + water complemented

NT: No treatment

L+miR: Leaf + miRNA duplex complemented

L+W: Leaf + water complemented

Synopsis

Title: Cross-kingdom affairs: Can microRNAs of host plants regulate genes of their insect herbivores?

Name: Rutwik Bardapurkar

Registration number: 20152009

Name of supervisor: Dr. Sagar Pandit

Department: Biology

Date of registration of Ph.D.: 1st August, 2017

Date of registration of Int. Ph.D.: 1st August, 2015

Institute: Indian Institute of Science Education and Research (IISER), Pune, India

---

Plants fend off their insect herbivores using chemical defenses. Various herbivory-induced plant molecules exhibit insecticidal effects upon ingestion by herbivores. Several small RNAs, including microRNAs (miRNAs), are also induced in plants after herbivory. Commonly, small RNAs play a role in the post-transcriptional gene regulations within their cell or tissue of origin. Since the herbivore ingests the leaf's herbivory-induced small RNAs, we hypothesized that they regulate its gene expression. We used miRNA as a small RNA model to test this hypothesis.

First, we experimentally tested the ingested miRNA-mediated gene regulation as a proof of concept in *Plutella xylostella* using its own let-7 miRNA. Pre-let-7 and mature-let-7 feeding led to target downregulations. Larvae also showed growth and developmental defects, validating the functionality of the trophically acquired miRNA. Then, we tested the hypothesis that the host plant's miRNAs regulate the herbivore's genes. *Arabidopsis thaliana* and *P. xylostella* were used as host plant and insect herbivore models, respectively. The hypothesis was tested using both *silico* and experimental approaches.

In the *in silico* analysis performed with three different target prediction algorithms, 128 plant miRNA-target insect mRNA pairs (CP), including 51 plant miRNAs, were common. Due to pre- and mature [double-stranded (ds)]- forms of miRNAs in the herbivore-ingested leaf, we analyzed whether the insect's miRNA machinery can process them. Our results suggest that the mature CP miRNAs have structural features similar to positive control *P. xylostella* and AGO-1-binding *Drosophila melanogaster* miRNAs (positive controls). Next, we identified the *Px*-Dicer-1 with an insect Dicer-1 hallmark,

the absence of the DECH motif in the N-terminal DEAD domain. More importantly, 3D modeling showed high structural similarity between the plant (*Ath*-Dicer-like-1) and insect (*Px*-Dicer-1) dicer-1s. Helicase and PAZ domains assess pre-miRNAs' loop and stem length to form the mature duplex. The average pre-miRNA, stem, and loop lengths in CP and *P. xylostella* miRNAs were similar. Further, the dicing site distributions of CP and *P. xylostella* miRNAs were similar, hinting that the CP miRNAs were amenable to cleavage by *Px*-Dicer-1. Thus, the *in silico* analysis indicated that the insect miRNA processing pathway can process plants' pre- and mature miRNAs.

For the empirical validation, we first analyzed the response of CP miRNAs to herbivory. Thirteen CP miRNAs were induced after 1 h of herbivory and jasmonic acid (JA) application, the 'plants' lepidopteran herbivory response indicator. Three CP miRNAs, *ath*-miR-164, *ath*-miR824, and *ath*-miR447, were found to target glucosinolate sulfatase (*GSS*), *P. xylostella*'s counter-defense against *A. thaliana*'s prime defense, the glucosinolate-myrosinase system. We selected this target gene for further study. Larvae fed on *ath*-miR164, *ath*-miR824, and *ath*-miR447 showed 5.9-fold, 10.2-fold, and 4.9-fold reductions in *GSS* transcripts, respectively. As *ath*-miR164 showed continuous induction upon herbivory, we selected it as a candidate. When the larvae were fed pre- and mature-*ath*-miR164 via a glucosinolate-replete diet, they showed 3.2- and 3.5-fold higher mortality, 2.5- and 2.7-fold longer first instar duration, and 1.55- and 1.44-fold lower mass than controls, respectively. Such an effect was not observed when these miRNAs were fed via a glucosinolate-deplete diet. Glucoraphanin, *A. thaliana*'s major glucosinolate, was reduced by >3.1 folds in the *ath*-miR164 fed larvae than controls; similarly, desulfoglucoraphanin, larvae's glucoraphanin-detoxification product, was reduced by >6.9-folds. Sulforaphane, the insecticidal product, increased >5.5-fold *ath*-miR164-fed larvae than the controls. These results suggested that 'larvae's differential fitness was associated with their differential glucosinolate detoxification efficiencies.

Last, we studied the *ath*-miR164-mediated *GSS* downregulation's ecological role by analyzing *P. xylostella*'s natural enemies' preferences towards and performances of the *ath*-miR164-fed larvae. We found that two major natural enemies, *Diadegma semiclausum* (parasitoid) and *Chrysoperla carnea* (predator), do not show a differential preference for the *ath*-miR164-fed larvae. However, we found that *D. semiclausum* larvae showed >8.7-fold mortality in the pre-and mature-*ath*-miR164-fed *P. xylostella* larvae than controls. Parasitoid mortality was not observed when pre- and mature- *ath*-miR164

were fed via a glucosinolate-deplete diet, suggesting that the mortality was associated with the isothiocyanate content of the *P. xylostella* larvae.

Together, this study provides *in silico* and empirical evidence of plant 'miRNAs' cross-kingdom role in plant defense against an insect herbivore.

Chapter I

Introduction

1. Introduction

The evolutionary arms race best defines the plant-herbivorous insect interaction. Both the taxa keep evolving adaptations and counteradaptations against each other to attain the one-upmanship. Plants respond to insect attacks by producing defensive secondary metabolites and proteins, against which the insects evolve counter-adaptations like detoxification, sequestration and rapid excretion (Schuman & Baldwin, 2016, Després et al., 2007).

Plants have several layers of defense systems against herbivores (Erb & Reymond, 2019). The chronology of events that mount plants' defense can be observed after the insect attack is perceived. Defense is initiated with the influx of cytosolic Ca^{2+} ions within seconds after the insect attack. Lepidopteran herbivory or mechanical wounding on *A. thaliana* leaf can induce Ca^{2+} within 2s (Toyota et al., 2018). This signal spreads to distal leaves within 2 min. Apart from the calcium response, reactive oxygen species (ROS) and electrical signals also mount local and systemic defense (Choi et al., 2017). The downstream Ca^{2+} ion signaling occurs via calcium sensors such as Calmodulin and Calcium-dependent protein kinases, which further activate transcription factors involved in Jasmonate (JA) biosynthesis (Scholz et al., 2014). ROS and reactive nitrogen species can be detected minutes to hours after herbivory. ROS (H_2O_2) is induced upon membrane depolarization by activating various oxidases (Drerup et al., 2013). The role of ROS *in planta* includes the activation of lipoxygenases involved in JA biosynthesis, while its ingestion can directly act on the feeding herbivore. Similarly, nitric oxide (NO) produced through Ca^{2+} influx is also involved in JA-mediated defense by activating NO-associated protein-1 and nitroso-glutathione pathway, which induces JA-mediated defense (Mur et al., 2013). Although a defense molecule, some insects have evolved quenching proteins against H_2O_2, thus reducing its effect (Zebelo & Maffei, 2015). These events summarize the early defense responses that prime plants.

The central molecules involved in activating and regulating plant defense apart from JA are salicylate (SA) and ethylene. JA is involved in defense against most chewing insects, including beetles and caterpillars, while SA-mediated response is shown to be induced by some aphids and whiteflies only (Wang et al., 2019b). JA biosynthesis begins ~1-2 h after herbivory (Schmelz, 2015). The functional form of JA is JA-Ile, a positive regulator of ~71 *A. thaliana* transcripts, many of which (especially the glucosinolate biosynthesis genes) are involved in plant defense (Bodenhausen & Reymond, 2007). Defensive

secondary metabolites regulating genes are downstream of the JA-Ile signaling (Benevenuto et al., 2019, Pérez-Alonso et al., 2021, Boter et al., 2004). Plants also produce insect-protease inhibitors, induced hours to days after herbivory (Giri et al., 2006). Other induced genes include enzymes involved in defensive secondary metabolites biosynthesis (Kessler, 2015), which may take hours to days after herbivory (Maffei et al., 2007).

Apart from plants' metabolite and protein-based defense induction, several studies have implicated the role of small regulatory RNAs (sRNAs) (Fig. 1) in plant defense against pathogens and insect herbivory (Kumar et al., 2022, Rabuma et al., 2022, Ražná & Cagáň, 2019). The two major classes of sRNAs are short-interfering RNAs (siRNA) and microRNAs (miRNAs). siRNAs (18-24 nucleotide long) are produced from long dsRNAs, whereas miRNAs (21-24 nucleotide long) are encoded by their genes (Zhu & Palli, 2020, Vogel et al., 2019).

miRNAs function primarily by regulating messenger RNA transcripts. miRNAs are formed from independent loci or are part of a protein-coding gene. Mechanistic details of primary miRNA transcript formation and its processing have been discussed before (Carthew & Sontheimer, 2009, O'Brien et al., 2018). In plants, primary miRNA transcripts are processed by Dicer-like proteins, especially DCL1, to form a hairpin pre-mature miRNA (pre-miRNA) intermediate. Another round of cleavage forms a 21-24 nucleotide miRNA duplex transported to the nucleus (Bajczyk et al., 2023, Wang et al., 2019a). In animals, including insects, the two cleavages are carried out by Drosha and Dicer-1 for primary miRNA and pre-miRNA, respectively. The pre-miRNA is transported to the cytoplasm for Dicer-1-mediated processing. In plants and animals, miRNA strands from the duplex are selected and loaded onto Argonaute (AGOs) (Dexheimer & Cochella, 2020, Vorozheykin & Titov, 2020). Many accessory proteins are involved in Dicer to AGO handover and the function of AGO-associated RNA-induced silencing complex (Kim & Kim, 2012, Pratt & MacRae, 2009, Zhang et al., 2018). Depending on the AGO, the RISC can carry out mRNA strand cleavage or block mRNA translation (Iwasaki et al., 2009).

Various plants show miRNA induction minutes to hours after the onset of herbivory. Several *N. attenuata* miRNAs were induced after *Manduca sexta* herbivory, 1-5 h after simulated herbivory (Bozorov et al., 2012). Similarly, *Solanum lycopersicum*, *Solanum habrochaites* (Wang et al., 2018a), *Camelia chinesis* (Jeyaraj et al., 2017), *Oryza sativa* (Wu et al., 2017), *Cucumis melo* (Sattar et al., 2012), and *Chrysanthemum morifolium*

(Xia et al., 2015) also show miRNA induction in response to insect herbivory. Interestingly, miRNA induction occurs before defensive secondary metabolite production (Fig. 2a). Several miRNAs are involved in plant defense pathways (Pandey et al., 2008, Sattar et al., 2012). For example, eight rice miRNAs integrate immune and physiological responses that affect grain yield (Kumar et al., 2022).

The two intermediates in the miRNA pathway (Fig. 1), the pre-miRNA and the mature miRNA duplex are double-stranded (ds) in nature. Unlike miRNAs, long dsRNAs in the siRNA pathway are diced by Dicer-2 to form 18-24 nucleotide dsRNAs that can cause RNA interference (RNAi). This phenomenon has been widely used in reverse genetic studies to study gene function. Since the discovery of RNAi, wide-scale studies have shown the presence of the RNAi machinery in almost all eukaryotes (Min & Lee, 2007). RNAi can occur via miRNA, siRNAs, and other classes, although their biogenesis and RNAi pathways differ. In the siRNA biogenesis pathway, long dsRNA diced by Dicer-2 creates multiple tandem dsRNAs, which can target multiple complementary mRNAs, causing RNAi in multiple genes. In contrast, pre-miRNA produces only a few target-specific mature miRNAs, suggesting that miRNA-mediated gene regulation has evolved to be target-specific (Kehl et al., 2017).

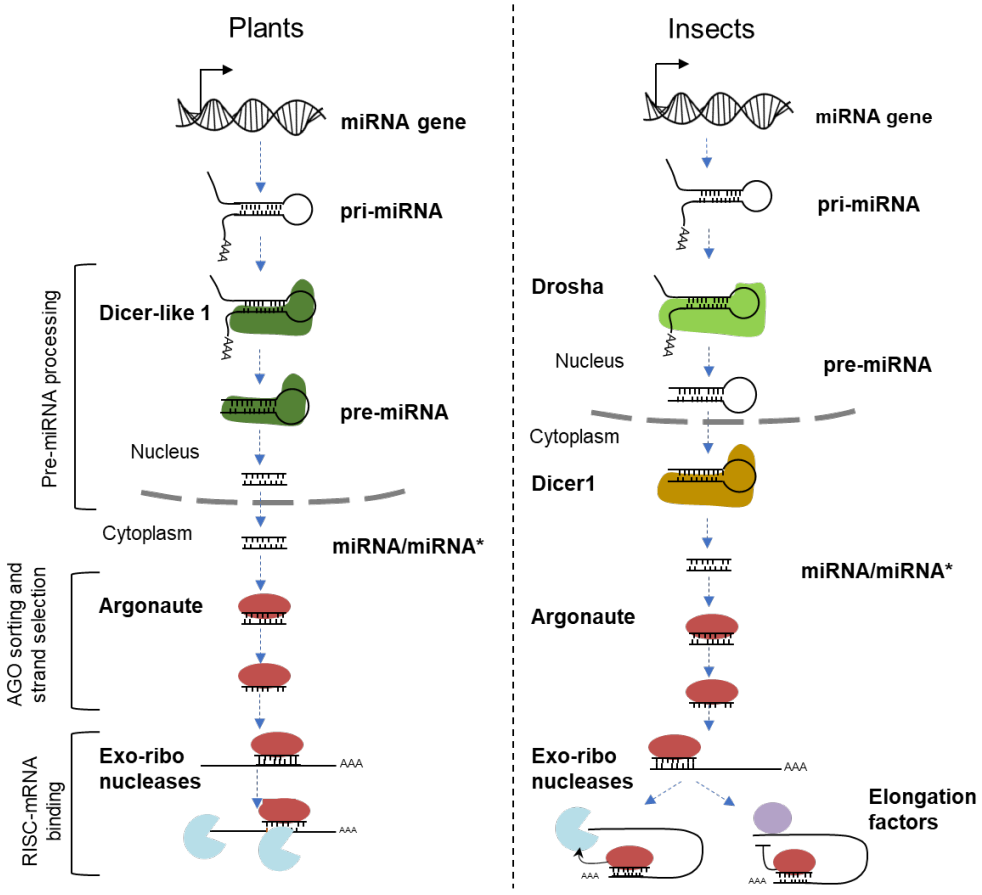

Figure 1 microRNA (miRNA) biogenesis and regulation in plants and insects | Genes encode primary miRNAs with internal stem-loop regions. In plants, Dicer-like 1 is primarily involved in processing the primary miRNA into pre-miRNA and further into mature miRNA duplex. Duplexes are sorted and handed over to Argonaute, forming the RISC. Argonaute selects the functional strand as the guide strand, and the complementary strand is degraded. The plant and insect miRNA pathways are conserved despite several differences. In insects, primary miRNAs are processed by Drosha to form pre-miRNA, which is exported out of the nucleus. Dicer-1 is involved in the processing of pre-miRNAs to form mature miRNA duplexes. The RISC binds to the target mRNA, leading to post-transcriptional gene regulation via mRNA cleavage by exo-ribonucleases (prominent in plants) or translational repression by blocking elongation factor (prominent in insects).

Trophically delivered or injected exogenous dsRNAs showed RNAi effect in *C. elegans* (Timmons et al., 2001). Herbivores feeding on host plants engineered to produce insect-origin siRNAs showed reduced expression of target mRNAs (Knorr et al., 2018, Kumar et al., 2012, Mao et al., 2007). Another study demonstrated that plants engineered to produce insect-origin pre-miRNAs could specifically target insect mRNAs (Bally et al., 2020). This plant-mediated RNA interference (PMRi) strategy is used for pest management and reduction of crop damage (Zotti & Smagghe, 2015) (Fig. 2b). Both these studies imply that dsRNAs (either RNA duplex or hairpin RNAs) are stably transferred from plant tissue to the insect gut and are functional in the gut tissue.

sRNAs usually target their target transcripts within the producer's cells. Considering the sRNA, especially miRNA production in herbivory-induced plants and the engineered plant-origin dsRNA uptake and action in feeding insects, we hypothesized that the hostplant's own miRNAs regulate insect herbivore's gene expression upon co-injection with the plant tissue (Zhang et al., 2019) (Fig. 2c).

The major siRNA pathway proteins, such as RNA-dependent RNA polymerase (RdRP), are still undiscovered in lepidopteran insects (Tomoyasu et al., 2008, Mamta & Rajam, 2017). However, the miRNA machinery is thoroughly characterized (Doench et al., 2003, Gordon & Waterhouse, 2007). In fact, Doench et al. showed that the miRNA machinery processed exogenously acquired siRNAs in the lepidopterans (Doench et al., 2003). Given that the miRNA genes, their targets, and the miRNA machinery are conserved, the miRNA pathway could be the major evolutionarily selected pathway in such insects (Obbard et al., 2006). Given the target-specific miRNA function, their cross-kingdom activity is a naturally developed mechanism in the plant-insect interaction (Zhang et al., 2019).

Trophical delivery of insects' own miRNAs can cause a target transcript reduction (Etebari et al., 2018). For example, trophically acquired miRNAs hampered larval growth, affected molting in *Spodoptera exigua* (Zhang et al., 2015), and increased larval deformity and adult mortality in *Helicoverpa armigera* (Saini et al., 2018). In *Bombyx mori*, several ingested miRNAs determine larval development, pupal maturation, and adult emergence (Yu et al., 2008). Trophically delivered miR-34-5p targets the ecdysone receptor, leading to high mortality, low fecundity, and developmental defects in several insects (Li et al., 2023). Even pre-miRNAs with engineered target binding cassettes overexpressed in plants targeted the *H. armigera*'s acetylcholinesterase transcripts (Bally et al., 2020). This indicates the active function of trophically acquired miRNAs. The double-stranded (ds) RNAs are highly stable in the gut lumen compared to their highly labile single-stranded forms (Zhang et al., 2021). Therefore, mature miRNAs' ds forms are active in the trophically acquired RNA pool. Hence, these ds forms are often used in trophic delivery studies (Zafar et al., 2021, Li et al., 2023).

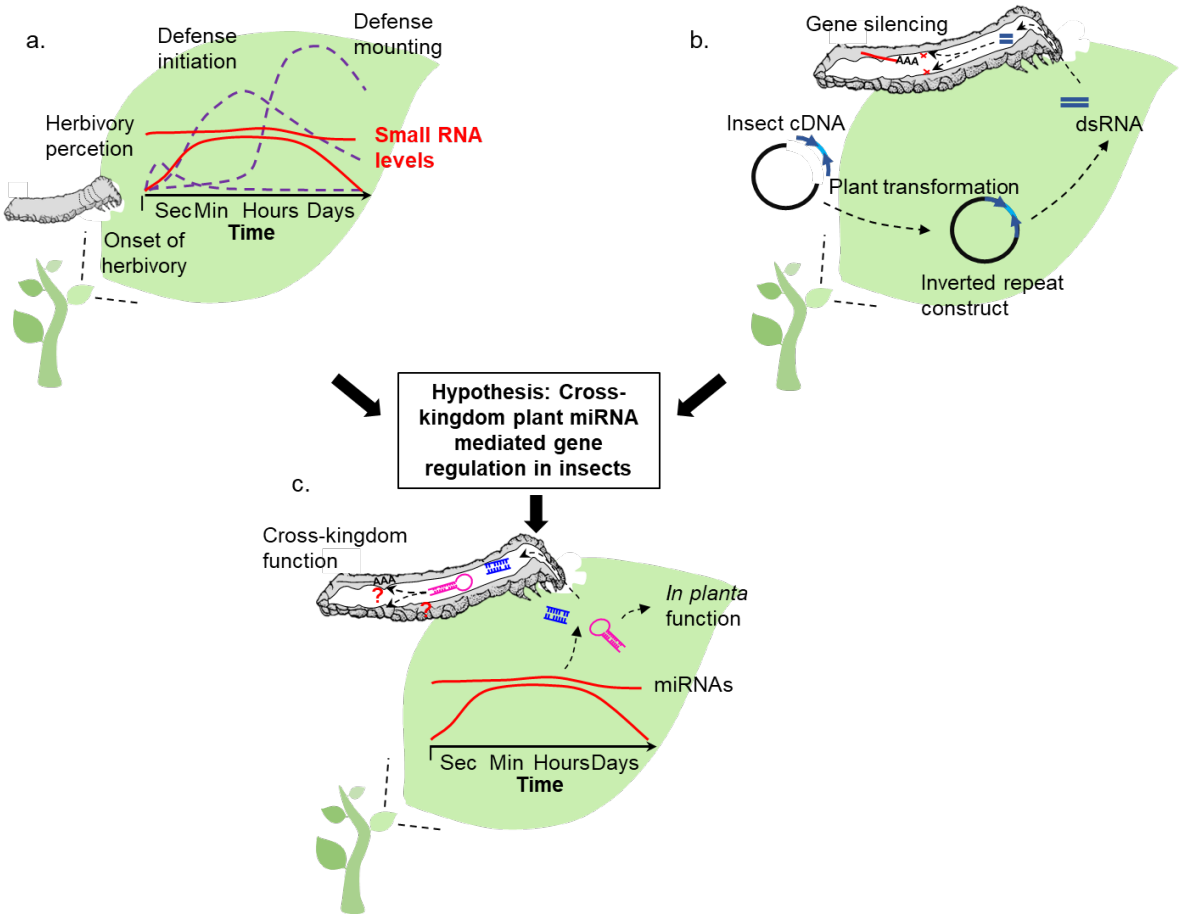

Figure 2 The molecular and ecological basis of cross-kingdom miRNA mediated gene regulation between plants and herbivorous insects | a. Chronology of plant molecular events upon herbivory as a function of time. Representative induction of miRNAs is presented in red. **b.** Synthetically generated sRNAs from plants can regulate insect gene expression. As a novel technique for pest control, plant-mediated RNA interference (PMRi) refers to artificially engineering host plants to produce insect-specific dsRNAs. These trophically acquired dsRNAs can stably transfer through the gut barrier when the pest feeds on the plant and regulate gene expression. **c.** The study's hypothesis: Naturally present plant sRNAs and their putative cross-kingdom roles in gene expression regulation. Based on the induction of sRNAs in plants upon herbivory and PMRi, we suggest that the naturally present plant sRNAs may be an additional means by which plants and insects interact. sRNAs, whether constitutively present or induced upon herbivory apart from their *in planta* role, may also cross the gut barrier of insects upon ingesting leaf tissue and regulate insect gene expression.

The primary necessity of this study is to have a plant-insect system with available information on plant miRNAs and insect mRNAs. We chose to study *A. thaliana* (L.) Heynh. (Brassicales: Brassicaceae), and *Plutella xylostella* L. (Diamondback moth) (Lepidoptera: Plutellidae) as the plant-insect system and also studied *P. xylostella*'s natural enemies, *Diadegma semiclausum* Hellén (Hymenoptera: Ichneomonidae) and *Chrysoperla carnea* Stephens (Neuroptera: Chrysopidae). *P. xylostella* is a specialist lepidopteran insect of the Brassicaceae family of plants. It is a notorious pest, with an economic cost between US$ 4-5 billion per year for its control (Zalucki et al., 2012, Fathipour & Mirhosseini, 2017, Li et al., 2021). miRNAs are extensively studied in *P. xylostella,* especially in characterizing miRNA targets involved in detoxification or insecticide resistance (Li et al., 2015, Wei et al., 2016, Ma et al., 2017, Morin et al., 2017, Zhu et al., 2017, Li et al., 2020). Moreover, *P. xylostella* uptakes *A. thaliana* miRNAs that potentially target its own transcripts (Zhang et al., 2019). Collectively, along with its agricultural importance, it is an important insect to study plant miRNA's function. The most extensively studied natural host of *P. xylostella* is *A. thaliana* (Handley et al., 2005). Due to the extensive genetic resources available in *A. thaliana*, the interaction between *P. xylostella* and *A. thaliana* system is a suitable system to study natural miRNA uptake and function.

In this study, we have systematically studied the uptake, function, and effects of *A. thaliana*-origin miRNAs in *P. xylostella*. Using the model miRNA let-7 (Liang et al., 2013), a highly conserved (Lee et al., 2016, Roush & Slack, 2008) miRNA critical in larval development, we first tested if miRNAs are functional in *P. xylostella* after dietary ingestion. In *Bombyx mori*, *Bm*-let-7 targets, *FTZ-F1,* and *E74* are ecdysone pathway

regulators responsible for larval instar transition (Liu et al., 2007, Ling et al., 2014, Song & Zhou, 2020). Their downregulation shows larval-larval and larval-pupal developmental arrests. Due to let-7's conserved nature and tractable phenotypes after target silencing, we tested the post-ingestion levels of *Px*-let-7 larval midgut and the effects on *Px-FTZ-F1* and *Px-E74* transcripts. We also studied the effects of let-7 ingestion on larval development and mortality.

To test plant miRNA function, we first identified putative *A. thaliana* miRNA targets on *P. xylostella* mRNAs. We selected miRanda (Enright et al., 2003), RNA22 (Miranda et al., 2006), and RNAhybrid (Krüger & Rehmsmeier, 2006) algorithms for target site prediction in the transcriptome. These algorithms were selected based on the target organisms for which they were designed. MiRanda was initially used to predict *Drosophila melanogaster* miRNA targets, although it has recently been widely used in other systems. MiRanda uses a scoring scheme for every base pair, assigning a specific score and penalty. Being specifically made for insect target prediction, and given that the miRNA pathway is conserved across insects, MiRanda is a vital prediction tool to be included. We first tested the trophic delivery of miRNAs in *P. xylostella* and studied the compatibility of *A. thaliana* miRNAs with *P. xylostella's* miRNA biogenesis machinery. Later, we studied the cross-kingdom activity of *A. thaliana*'s *ath*-miR164 in regulating *P. xylostella*'s detoxification gene *Glucosinolate sulfatase* (*GSS*). Glucosinolates are pre-toxins physically segregated in leaf tissues from the enzyme myrosinase (Frerigmann et al., 2012). Wounding, followed by tissue rupture, leads to the action of myrosinases on the glucosinolates, converting them into toxic isothiocyanates. GSS desulfates glucosinolate, and the desulfo- form can no longer act as a substrate for myrosinases to form the isothiocyanate toxins (Chen et al., 2020). RNA22 is used across all the animal systems (Miranda et al., 2006). RNAhybrid has a broader usage, allowing plant and animal studies (Krüger & Rehmsmeier, 2006). It provides other parameters, such as target site abundance-based *p*-value restrictions, helix constraints, and internal-loop size. RNA22 does not look at target conservation and includes all mRNA regions, including 3' UTR, 5'UTR, and CDS. Analysis was restricted to animal-specific algorithms as the targets were from *P. xylostella*. We discover that *ath*-miR164 induces rapidly in the plant upon herbivory and affects *GSS1* levels, thereby attenuating the detoxification capability and, consequently, influencing the ecological interactions of *P. xylostella*.

Chapter 2

Materials and Methods

2. Materials and Methods

2.1. *In silico* target prediction

We used miRNA-target algorithms to predict *A. thaliana* miRNA targets in *P. xylostella.* All known *A. thaliana* miRNAs [MiRBase (release 22.1)] (Kozomara et al., 2019) were screened against the *P. xylostella* mid-gut transcriptome (3505 5'-UTRs, 2136 CDSs and 5702 3'-UTRs) [InsectBase (Mei et al., 2022)] for the presence of putative *A. thaliana* miRNA target sites in the *P. xylostella* mRNAs. For miRanda, targets with a >100 score and minimum < -25 kJ/mole free energy predictions were selected. These parameters were set according to previously reported target prediction in *P. xylostella*'s miRNAs (Etebari & Asgari, 2016). The common miRNA-target pairs (CP) showing identical binding sites (exact base-to-base alignment) predicted by all three target prediction algorithms were used as high-confidence miRNA-target pairs. Functions of the filtered mRNAs were predicted using the Gene Ontology prediction analysis (Thomas et al., 2022). BLAST2GO was used to assign GO terms to gain insight into the putative functions of the identified miRNA-target pairs (Ashburner et al., 2000).

2.2. Phylogenetic analyses

We constructed a phylogenetic tree to identify *P. xylostella*'s Dicer-1 and AGO (miRNA pathway component). For *P. xylostella*, Dicer or Dicer-like and AGO protein sequences were obtained from the 'Diamondback moth database' (Tang et al., 2014) and the *Homo sapiens*, *Acyrthosiphon pisum*, *Tribolium castaneum, Drosophila melanogaster, Anopheles gambiae, Aedes aegypti, Bombyx mori, Spodoptera litura,* and *A. thaliana* Dicer and AGO proteins from the NCBI database. Multiple sequence alignment was performed using MEGA7 (Kumar et al., 2016) with the CLUSTAL W algorithm (Thompson et al., 1994). Phylogenetic analysis of putative proteins from *P. xylostella* and annotated proteins from other insect systems was performed using Phylogeny.fr using the default parameters. The model utilizes the phyML 3.0/ aLRT algorithm with the HKY85 substitution model (Dereeper et al., 2008). This model has been widely recommended model for phylogeny building (Zardoya, 2021). The tree was constructed using the maximum likelihood method with a bootstrap value 1000.

2.3. Protein structure prediction

We used structural prediction tools to understand the structural similarities between plant and insect proteins. The three-dimensional structure of the Dicer-1 protein could not be

predicted using both homology-based or *ab initio* algorithms because of the unavailability of the well-elucidated template and the large protein size (2693 amino acids). *Ab initio* structure prediction methods lack accuracy and reliability for large proteins. Therefore, predictive homology-based modeling tools constructed the 3-dimensional structures of 8 characteristic domains of Dicers from *P. xylostella*, *D. melanogaster,* and DCLs from *A. thaliana*. Putative sequences were examined for domains essential for the Dicer function. Three different domain prediction servers viz. NCBI domain search (Lu et al., 2020), SMART (Letunic & Bork, 2018), and Prosite (de Castro et al., 2006) were used to identify domains. The consensus sequence identified from all three prediction tools was used for further analysis. SwissModel (Waterhouse et al., 2018), ModWeb (Eswar et al., 2003) , and Phyre2.0 (Kelley et al., 2015) were used to build domain structures. SwissModel uses two database search methods- HHblits and BLAST to obtain a more accurate template. The algorithm considers different highly-ranked target-template alignments and gives multiple predicted structures. ModWeb uses query sequence-structure alignment with the template by PSI-BLAST to finalize the template/s. The phyre2.0 algorithm pipeline is very similar to SWISS-Model but includes an additional step of secondary structure prediction prior to modeling. Considering the variation in the approach of algorithms, we used all of them to predict biologically relevant domain structure. Default parameters from the servers were used. The output structures of the Dicer domains of *P. xylostella* and *D. melanogaster* were superimposed with *A. thaliana* using the RMSD-based structural superimposition method. All possible combinations of structures given by different algorithms were compared using UCSF Chimera (Pettersen et al., 2004).

As a proxy for functional conservation, protein level similarity between AGO structures, *P. xylostella* AGO-1, and AGO-2 was predicted and superimposed with *D. melanogaster* AGO-1 and AGO-2 structures. An average sequence length of 1031 amino acids allowed homology-based modeling similar to Dicer.

2.4. Analysis of pre-miRNA structures

To determine whether foreign pre-miRNAs can function in an insect system, it is necessary to ensure that the pre-form is compatible with the insect Dicer. *A. thaliana*, *P. xylostella*, and *D. melanogaster* pre-miRNA sequences were obtained from the miRBase. The secondary structure generated by RNAfold (Lorenz et al., 2011) using default parameters was used to calculate the loop and stem length (5' and 3') for every miRNA. For measuring loop length, the first base with ≤ 0.5 binding probability near the loop was

considered the first base of the loop. The stem length (5' or 3') was measured from the respective ends to the last paired base, which had a> 0.5 probability of binding. Lengths of pre-miRNAs for *P. xylostella* (*Pxy*-pre) were compared with *D. melanogaster* (*Dme*-pre), pre-miRNAs from the common miRNA-target pairs from *in silico* target prediction analysis (CP-pre) and remainder pre-miRNAs (nCP-pre) pre-miRNAs from *A. thaliana*. We also compared the dicing position of pre-miRNAs. Since two different proteins, viz. DCL and Dicer-1 are involved in pre-miRNA dicing in the plant and insect systems; insect Dicer-1 cleavage preference can determine *A. thaliana* pre-miRNA dicing sites. For this comparison in the pre-miRNA stem, pre-miRNA bases from the 5' end were counted up to the first base of the mature strand, or the bases from the 3' end were counted up to the last base of the star (miRNA*) strand.

2.5. Classification of AGO-1 vs. AGO-2 loading miRNAs

To determine whether foreign mature miRNAs can function in an insect system, it is necessary to ensure that the mature miRNA duplex is compatible with the insect AGOs. Doench et al. showed that exogenously acquired siRNAs are processed via the mina pathway (Doench et al., 2003). To analyze whether plant mature miRNA duplexes load on AGO-1 or AGO-2, we compared the miRNA loading features between *A. thaliana*, *P. xylostella* miRNAs, and known AGO-1- and AGO-2-loading miRNAs from *D. melanogaster* (Ghildiyal et al., 2010, Kawamura et al., 2008). Previously reported three independent features of a mature miRNA duplex (miRNA/miRNA*), the terminal end stability, 5'-terminal nucleotide identity, and mismatches in the central region (8-11 nucleotides) of the duplex were used (Ghildiyal et al., 2010) (Fig. 13a).

The miRNA/miRNA* duplexes were obtained from the sequences annotated in miRBase. Base pair pairing probabilities of each duplex were calculated using RNAcofold (Bernhart et al., 2006) to obtain miRNA loading features. We correlated the central (base 8-11) and terminal base pairing probabilities and 5' nucleotides between *P. xylostella* (*Pxy*), known *D. melanogaster* AGO-1 binding miRNAs (*Dme*-AGO-1-md), known *D. melanogaster* AGO-2 binding miRNAs (*Dme*-AGO-2-md), filtered *A. thaliana* (CP-md), and unfiltered *A. thaliana* (nCP-md) miRNA duplexes (Ghildiyal et al., 2010). Experimentally validated *D. melanogaster* miRNAs known to load on AGO-1 [(*dme*-bantam, *dme*-let-7, *dme*-miR-4, *dme*-miR-9c, *dme*-miR-14, *dme*-miR-34, *dme*-miR-133, *dme*-miR-219, *dme*-miR-274, *dme*-miR-275, *dme*-miR-277, *dme*-miR-278, *dme*-miR-280, *dme*-miR-281-1, *dme*-miR-282, *dme*-miR-303, *dme*-miR-310, *dme*-miR-994, *dme*-

miR-1000) (n= 19)] and AGO-2 [(*dme*-miR-8, *dme*-miR-10, *dme*-miR-11, *dme*-miR-13b-1, *dme*-miR-13b-2, *dme*-miR-79*,* *dme*-miR-92b, *dme*-miR-308, *dme*-miR-20072) (n= 9)] were used as positive controls (Kawamura et al., 2008).

2.6. Plant and insect maintenance

Wild-type *A. thaliana* (Col-0) seeds were germinated on Murashige and Skoog medium, and the seedlings were transferred to the soil after three weeks. Soil comprised equal proportions of red soil, vermiculite, perlite, and coco peat. Plants were maintained in the growth chambers at 21 °C, 60 % relative humidity, and under 10 h light/ 14 h dark cycles. Two-month-old rosettes were used for all experiments.

P. xylostella was maintained by feeding the larvae on an artificial diet (AD) at 24 °C, 70 % relative humidity, and a 16:8 h light: dark photoperiod (Shelton et al., 1991). Adults were fed using the 10 % sucrose solution-soaked cotton pads. Larvae from the fourth generation of the culture were used in all the experiments.

2.7. Time-course miRNA induction assay

To find whether these *in silico*-identified miRNAs are herbivory-associated, we analyzed their temporal expression after herbivory. 20 neonates were fed per leaf (two-month-old plants) for the 0, 1, 6, 12, 24, and 48 h intervals. Leaf tissue (Hb) was harvested and flash-frozen at appropriate intervals in liquid nitrogen. To control for sporadic larval feeding and allow precision in induction time, a fabric pattern wheel was used to wound on each side of the midrib, and 10 µl 10× diluted *P. xylostella* oral secretion (W+OS) was applied to the wounds. Pattern wounding along with 10 µl MilliQ was used as a control (W+W) along with an untreated control (NT). From the 51 CP miRNAs (31 miRNA families) identified from the *in silico* target prediction analysis, twenty-two miRNAs had unique sequences, allowing for quantitation, and were analyzed using qPCR.

2.8. *In vitro* transcription

In vitro transcribed miRNA duplexes or pre-miRNAs were utilized for all miRNA feeding assays. Pre-let-7, let-7, *ath*-miR164c (referred to as *ath*-miR164), *ath*-miR447c (referred to as *ath*-miR447), and *ath*-miR824 were synthesized using the DNA templates with upstream T7 promoter sequences (Table 1). For the let-7 ingestion experiments, four forms, viz. pre-let-7, pre-let-7 negative control (pre-C) with a scrambled seed sequence, mature ds let-7, and its negative control (mature-C) with a scrambled seed sequence, were used. For all mature double-stranded (ds) miRNAs, both strands were independently

transcribed and stored at -20 °C. Transcription reactions were performed according to Donze and Picard (2002). Each reaction (50 µl) contained 200 pmol DNA, 1 mM rNTPs, 40 mM Tris–HCl pH 7.9, 6 mM MgCl2, 10 mM DTT, 10 mM NaCl, and 2 mM spermidine, 100 U T7 polymerase, and 40 U recombinant Ribonuclease inhibitor (Takara, Japan). After 4 h incubation at 37 °C, reactions were treated with 1 U DNAse (HiMedia, India). Both strands were reassociated by slow cooling and purified. miRNAs were hand-mixed and mixed with AD or complemented on *A. thaliana* leaves.

Table 1 Templates for *in vitro* transcription.

Template	**Sequence**
T7 promoter	TAATACGACTCACTATAGG
let-7 5p strand	CTATACAACCTACTACCTCACCTATAGTGAGTC GTATTA
let-7 3p strand	GGAAAGTTAGCAGGCTATACAGCCTATAGTGA GTCGTATTA
scrambled let-7 5p strand	CTATACAACCTTCCCATCTACCTATAGTGAGTC GTATTA
scrambled let-7 3p strand	GGAAGAAGAGCAGGCTATACAGCCTATAGTGA GTCGTATTA
pre-let-7	ACTGGCCAGGAAAGTTAGCAGGCTATACAGTC CCCCGTTCGGTGTAATACTGTACTATACAACCT ACTACCTCAGCTGGCCGAGCCTATAGTGAGTCG TATTA
scrambled pre-let-7	ACTGGCCAGGAAGAAGAGCAGGCTATACAGTC CCCCGTTCGGTGTAATACTGTACTATACAACCT TCCCATCTAGCTGGCCGAGCCTATAGTGAGTCG TATTA
ath-miR447c 5p strand	CAACAAAAGATGTCGTCCCCAATATAGTGAGT CGTATTA
ath-miR447c 3p strand	ATTAGCGGACACATGCTTTGTTATAGTGAGTCG TATTA
ath-miR164c 5p strand	CGCACGTGCCCTGCTTCTCCATATAGTGAGTCG TATTA
ath-miR164c 3p strand	GTTGGAGTAGTAGAACACGTGTATAGTGAGTC GTATTA
ath-miR824 5p strand	TCCCTTCTCACAAATGGTCTACTATAGTGAGTC GTATTA
ath-miR824 3p strand	TCTAGACCATCGATGAGAAGGCTATAGTGAGT CGTATTA

2.9. miRNA ingestion assay

We studied the effect of miRNA ingestion on larval transcripts. For the let-7 concentration standardization, 0, 4, 7, 10, 13, and 16 µg miRNA-supplemented diet was provided to larvae. For let-7 ingestion experiments, the 4 forms of 10 µg miRNAs (refer to section 2.8) were hand-mixed with AD and provided to larvae. All assays were conducted in 20 ml polypropylene containers. Larvae were dissected at 24 h. To test whether ingested let-7 levels affect target transcripts, we compared midgut transcript levels of *FTZ-F1* and *E74*. We also tested the levels of pre-let-7 and let-7 after miRNA ingestion. We also tested *Dicer-1*, *Dicer-2*, *AGO-1*, and *AGO2* transcript levels to understand if the sRNA pathway components are miRNA-responsive.

For studying *A. thaliana* miRNA ingestion-associated effects, we used a leaf substrate for miRNA delivery. Leaf substrate allowed us to study the effects of WT and aliphatic-glucosinolate *A. thaliana* mutants (also refer to sections 2.10-2.13). For the ingestion assay, 10 µg miRNA-complemented leaves (L+miR) were provided to larvae (Fig. 16a). Leaves complemented with water were used as control (L+W). Larvae were dissected at 0, 24, 48 and 72 h. Independent assays were conducted per replicate (n= 6, 20 larvae per replicate). Larvae were provided with a fresh diet every 12 h. For this study, We selected *GSS1* and *GSS2* targeting *ath*-miR164, *ath*-miR447, and *ath*-miR824, as GSS is *P. xylostella*'s primary counter-defense. We tested if trophically delivered *ath*-miR164, *ath*-miR447, and *ath*-miR824 affect *GSS1* and *GSS2* expression. We confirmed target specificity by studying the effect of *P. xylostella*'s own trophically delivered miRNAs, *pxy*-miR375, *pxy*-miR8534, and *pxy*-miR8533 levels on their reported targets, *CYP4G15*, *CYP6B6*, and, *LCP30*, respectively (Zhu et al., 2017). We confirmed target specificity, by feeding *ath*-miR164, *ath*-miR447, and *ath*-miR824 and analyzing *CYP4G15*, *CYP6B6*, and, *LCP30* levels. Of the three miRNAs, only *ath*-miR164 showed a continuous induction, and its dietary feeding showed continuous *GSS1* repression. Hence, we selected *ath*-miR164 for further studies. Larvae were fed with mature *ath*-miR164, *ath*-pre-miR164, or a *GSS1*-specific dsRNA-complemented (ds*GSS1*) on WT or *myb28myb29* plants (glucosinolate-deplete plant). *myb28myb29* is a double-knockout mutant of *myb28* and *myb29*, transcription factors involved in the aliphatic glucosinolate biosynthesis (Sønderby et al., 2007). As aliphatic glucosinolates constitute 85% of the total glucosinolate content, we used this mutant to delineate the effects of glucosinolates on miR164-mediated *GSS1* suppression. ds*GSS1* was a positive control for dietary *GSS1*

silencing (Sun et al., 2020). For the *ath*-miRNA ingestion experiment, we tested *GSS1* and *GSS2* transcript levels after *ath*-miR164, *ath*-miR447c, and *ath*-miR824 feeding. Larvae were dissected in 1× Tris-EDTA buffer (HiMedia, India). Insulin needles were used to cut the head and posterior end segments, and the midgut was pulled out. The midguts were stored in RNAiso Plus at -20 °C until further use.

2.10. *P. xylostella* performance assay

To understand the effects of let-7 ingestion on larval performance, we analyzed the first instar duration (n= 30), larval mass (n= 30), mortality (%) (n= 5, each set contains 100 larvae), and eclosion (%) (n= 5, each set contains 100 pupae). Mass and mortality were measured after 60 h. To assess the effect of *ath*-miR164 feeding on *P. xylostella* larvae, we analyzed first instar duration (n= 30), larval mass (n= 30), and mortality (%) (n= 5, each set contains 100 larvae). Larvae were fed on *ath*-miR164-complemented, pre-miR164-complemented, or dsRNA-complemented leaves. Larval mass and mortality were recorded after 24 h.

2.11. Natural enemy preference assay

We hypothesized that miRNA-mediated cross-kingdom effects on *P. xylostella's* detoxification ability could also further affect the third trophic level. To assess whether *ath*-miR164 ingestion affects *C. carnea*'s predation behavior, we provided *P. xylostella* fed on *ath*-miR164, pre-miR164, or ds-*GSS1*-complemented leaves to *C. carnea* (third instar). Water-complemented and untreated leaves were used as controls. In the choice setup, *C. carnea* larvae were allowed to choose between *P. xylostella* larvae fed on the different treatments in a 20-minute assay (n= 5, each set contained 20 *C. carnea* larvae). For the no-choice setup, individually treated *P. xylostella* larvae were provided to *C. carnea* (n= 5, each set contained 20 *C. carnea* larvae) in a 20 min assay. Similarly, *D. semiclausum* females were allowed to oviposit on *P. xylostella* larvae. *D. semiclausum* males and females were allowed to mate for 2 days before the assay. Larvae were presented to *D. semiclausum* females in no-choice and choice setups. Oviposition preference was counted until parasitization was observed in each assay (n= 5, each set contained 20 *D. semiclausum* wasps). *D. semiclausum* mortality was recorded after 48 h of ovipositioning (n= 5, each set contained 20 *D. semiclausum* wasps).

2.12. Natural enemy performance assay

To study the impact of *ath*-miR164 ingested- *P. xylostella* larvae on the performance of *C. carnea*, we assessed *C. carnea* mortality when continuously preying on *P. xylostella* fed on *ath*-miR164, pre-miR164 or ds-*GSS1*, water-complemented and untreated leaves from either Col-0 or *myb28myb29* backgrounds (n= 5, each set contained 20 *C. carnea* larvae). *C. carnea* larval mortality was measured after 48 h. Similarly, oviposited *D. semiclausum* was counted after 48 h, and mortality was measured (n= 5, each set contained 20 *D. semiclausum* wasps).

2.13. Metabolite quantitation in *P. xylostella* midgut

As *P. xylostella* larvae were negatively affected after feeding on RNA-complemented WT plants and not on *myb28myb29*, we hypothesized that the *GSS* transcript reduction impacted glucosinolate metabolism in larvae feeding on RNA-complemented WT plants. We tested this by analyzing glucoraphanin, desulfoglucoraphanin, and sulforaphane levels (n= 6, each set contains 50 larvae). *P. xylostella* midguts fed on different treatments were homogenized in 100 µl extraction buffer (60% methanol; pH 3, adjusted using acetic acid) for 3 min. Samples were centrifuged for 30 min at 14000 RPM at 4 °C. The samples were separated on a Phenomenex Gemini® C18 column (50x4.6 mm, 5µm,118Å) and analyzed on the SCIEX-X500R UPLC/ESI/QTOF-MS. A negative ion mode was utilized for glucoraphanin, and a positive ion mode was utilized for desulfo-glucoraphanin and sulforaphane. Selected parent ions were quantified by multiple reaction monitoring. All parameters were as previously reported (Sun et al., 2019).

2.14. RNA extraction, cDNA synthesis, and real-time PCR

Larvae were dissected (n= 5, each set contains 20 larvae), the isolated midguts were washed in the ice-cold Tris-EDTA buffer, and they were stored in 250 µl RNAiso Plus reagent (Takara, Japan) at 4 °C until use. 100± 20 mg flash-frozen leaf samples were mixed with 250 µl RNAiso Plus reagent and homogenized using glass beads. Total RNA was isolated using the manufacturer's instructions. RNA was precipitated overnight with sodium acetate and isopropyl alcohol (Rankem, India).

cDNA for all mRNA and pre-let-7 samples was synthesized using the PrimeScript Reverse Transcriptase kit (Takara, Japan). 100 ng RNA was used. For all miRNAs and 5S rRNA, 5 nM stem-loop primers were used for cDNA synthesis as previously described (Chen et al., 2005). qPCRs were performed using the SYBR Premix Ex Taq II reagent

kit (Takara, Japan) on the CFX96 Touch Real-Time PCR machine (Bio-Rad, USA). PCR thermocycling involved denaturation at 95 °C and 44 cycles of 95 °C-45 s, 60 °C-45 s and 72 °C-45 s. *Ubiquitin* was the internal reference transcript for all mRNAs and pre-let-7 and 5S rRNA for all miRNAs. All primers were designed in this study and are given in Table 2.

Table 2 Primers used for the cDNA synthesis and quantitative real-time polymerase chain reactions (qPCRs).

Sequence name	**Primer**	**Sequence**	**Used for**
ath-miR164c-5p	Stem-loop	CTTCTCCACTATGCTCTCCAGGTACA GTTGGTACCTGTCTCCACTTCGCACG	cDNA synthesis
ath-miR447c-3p	Stem-loop	CGTCCCCAACTCAACACGCCACCAG GTACAGTTGGTACCTGTAACACA	cDNA synthesis
ath-miR824-5p	Stem-loop	AGAAGGACACACACCAGGTACAGTT GGTACCTGACTCCACGCTCTAGACC A	cDNA synthesis
ath-miR165a-5p	Stem-loop	CAACATTCCATCCATGCAGGTACAG TTGGTACCTGTCTACACTTCCTC	cDNA synthesis
ath-miR169a-5p	Stem-loop	CATCCTTGATCCATGCAGGTACAGT TGGTACCTGTCTACACTTTCGGC	cDNA synthesis
ath-miR2934-3p	Stem-loop	CACCTTGACACACACCAGGTACAGT TGGTACCTGACACACACATTTCT	cDNA synthesis
ath-miR396b-5p	Stem-loop	TGGAATCACACACCAGGTACAGTTG GTACCTGCACACACAAGTTCAA	cDNA synthesis
ath-miR398a-5p	Stem-loop	ATCCTTATCCATGCAGGTACAGTTG GTACCTGGAACCTATTTGTGTT	cDNA synthesis
ath-miR414	Stem-loop	GAAGATGACACACACCAGGTACAGT TGGTACCTGACACACACATGAC	cDNA synthesis
ath-miR5023	Stem-loop	TACCAATACACACACCAGGTACAGT TGGTACCTGACACACACAGCCC	cDNA synthesis
ath-miR5634	Stem-loop	AAGTCCCTACACACACCAGGTACAG TTGGTACCTGACACACACACCCT	cDNA synthesis
ath-miR5660	Stem-loop	CCACCTGACACACACCAGGTACAGT TGGTACCTGACACACACATTCCA	cDNA synthesis
ath-miR771	Stem-loop	AGAGGCTACACACACCAGGTACAGT TGGTACCTGACACACACATGAGG	cDNA synthesis
ath-miR8165	Stem-loop	CCTCCATTACACACACCAGGTACAG TTGGTACCTGACACACACATCCTT	cDNA synthesis
ath-miR8173	Stem-loop	CAGCACATACACACACCAGGTACAG TTGGTACCTGACACACACATCCCA	cDNA synthesis
ath-miR8176	Stem-loop	ACCACCGCACACACACAGGTACAGT TGGTACCTGCAACCTATCCCT	cDNA synthesis
ath-miR8180	Stem-loop	CCGCACCACACACACCAGGTACAGT TGGTACCTGACACACACAGCACT	cDNA synthesis
ath-miR832	Stem-loop	GAATCAAACACACACCAGGTACAGT TGGTACCTGACACACACACTTGC	cDNA synthesis

ath-miR408	Stem-loop	AGTGCATCTATGTCCTCCAGGTACA GTTGGTACCTGTCTCACTGCCAGGG	cDNA synthesis
ath-miR8168	Stem-loop	GCACCTCACACACACAGGTACAGTT GGTACCTGCAACCTAGCACT	cDNA synthesis
ath-miR8171	Stem-loop	CACCTATACACACACCAGGTACAGT TGGTACCTGACACACACATCCTA	cDNA synthesis
ath-miR5661	Stem-loop	TACCTCCACACACACAGGTACAGTT GGTACCTGCAACCTACAGAC	cDNA synthesis
ath-miR164c-5p	Forward	AGCTTCTCCACTATGCTCTCCAG	qPCR
	Reverse	ATTGGAGAAGCAGGGCAC	qPCR
ath-miR447c-3p	Forward	CAACTCAACACGCCACCAG	qPCR
	Reverse	TGGGGACGACATCTTTTGTT	qPCR
ath-miR824-5p	Forward	GAAGGACACACACCAGGTACAG	qPCR
	Reverse	TTCTCATCGATGGTCTAGATGG	qPCR
ath-miR165a-5p	Forward	ACATTCCATCCATGCAGGTACA	qPCR
	Reverse	GCGGGAATGTTGTCTGGA	qPCR
ath-miR169a-5p	Forward	CATCCTTGATCCATGCAGGT	qPCR
	Reverse	AGCCAAGGATGACTTGCCG	qPCR
ath-miR2934-3p	Forward	CCTTGACACACACCAGGTACA	qPCR
	Reverse	CGCATCCAAGGTGTTTGTAGAAATG	qPCR
ath-miR396b-5p	Forward	TCACACACCAGGTACAGTTGG	qPCR
	Reverse	TCCACAGCTTTCTTGAACTTGT	qPCR
ath-miR398a-5p	Forward	ATCCATGCAGGTACAGTTGGT	qPCR
	Reverse	CCGCAAGGAGTGGCATGT	qPCR
ath-miR414	Forward	AGATGACACACACCAGGTACAG	qPCR
	Reverse	GCTCATCTTCATCATCATCGTCAT	qPCR
ath-miR5023	Forward	ACACACACCAGGTACAGTTGG	qPCR
	Reverse	GGCGATTGGTAGTGGATAAGGG	qPCR
ath-miR5634	Forward	TCCCTACACACACCAGGTACAG	qPCR
	Reverse	GGGACTTTGTGAATTTAGGGTGT	qPCR
ath-miR5660	Forward	CCTGACACACACCAGGTACAG	qPCR
	Reverse	CAGGTGGTTAGTGCAATGGAATGT	qPCR
ath-miR771	Forward	ACACACACCAGGTACAGTTGG	qPCR
	Reverse	TGAGCCTCTGTGGTAGCCC	qPCR
ath-miR8165	Forward	TCCATTACACACACCAGGTACA	qPCR
	Reverse	CCAATGGAGGCAAGTGTGAAG	qPCR
ath-miR8173	Forward	AGCACATACACACACCAGGTACA	qPCR
	Reverse	ATGTGCTGATTCGAGGTGGGATG	qPCR
ath-miR8176	Forward	ACCGCACACACACAGGTACA	qPCR
	Reverse	GCCGGTGGTCGCGAGAG	qPCR
ath-miR8180	Forward	CACCACACACACCAGGTACAG	qPCR
	Reverse	TGCGGTGCGGGAGAAGT	qPCR
ath-miR832	Forward	GAATCAAACACACACCAGGTACA	qPCR

	Reverse	ATTCCCAATCCAAGCAAGTG	qPCR
ath-miR5661	Forward	CCACACACACAGGTACAGTTGG	qPCR
	Reverse	GCCGCAGAGGTACATCATGTAG	qPCR
ath-miR408	Forward	AGTGCATCTATGTCCTCCAGGT	qPCR
	Reverse	CCTATAATGCACTGCCTCTTCC	qPCR
ath-miR8168	Forward	TCACACACACAGGTACAGTTGG	qPCR
	Reverse	GGTGCTGAGTGTGCTAGTGC	qPCR
ath-miR8171	Forward	TGGGGACGACATCTTTTGTT	qPCR
	Reverse	CAACTCAACACGCCACCAG	qPCR
GSS1	Forward	CATCAAGCTGTGGTGCTCCTC	qPCR
	Reverse	CTGCCGTCAAGCTGCTCC	qPCR
GSS2	Forward	CTGCATCAAGTAGTGGTGATTCTG	qPCR
	Reverse	GCTTGCCGTCAAGCCTCGAT	qPCR
FTZ-F1	Forward	CAAACTGGCCTCATGTCCCT	qPCR
	Reverse	TGGTAAGCTGCTCCTTGTGG	qPCR
E74	Forward	TCGACCTCTCCAATTGCCTG	qPCR
	Reverse	CGACAGTTCCCCGAGAGATG	qPCR
Dicer-1	Forward	TTGCTGCATGAGGACGCTTA	qPCR
	Reverse	TGAGGTCGTATGCCACACAC	qPCR
Dicer-2	Forward	TGATCTTCGACGAGTGCCAC	qPCR
	Reverse	CTATGGTGGCGTGGAAGGTT	qPCR
AGO1	Forward	CTCCATGATGTACACCCCGG	qPCR
	Reverse	GCTGGGCTTTGTAAAACGCA	qPCR
AGO2	Forward	GGAACTACTCTGAACCCGCC	qPCR
	Reverse	GATGAAAGGCCGGGAAGTGA	qPCR
Ubiquitin	Forward	CGTGAAGACCCTTACTGGCA	qPCR
	Reverse	TAGTCAGACAATGTGCGGCC	qPCR
Pre-let-7	Forward	GCCAGCTGAGGTAGTAGGTT	qPCR
	Reverse	ACTGGCCAGGAAAGTTAGCA	qPCR
Let-7	Forward	CCAGCTGGGTGAGGTAGTAGGTTGT	qPCR
	Reverse	CTGGTGTCGTGGAGTCGGCAATT	qPCR
5S rRNA	Forward	ACTGGATACGACAGCCAACG	qPCR
	Reverse	GGCGTGGTCAGTACTTGGAT	qPCR

2.15. Data analysis

Fold changes between two means, a and b, were calculated as $\left(\frac{a}{b}\right)$, where a > b. All data were tested for homogeneity of variance and normality. Levene's test was used to assess the homogeneity of variance between data (homogenous data). If the test statistic was < 0.05, the null hypothesis that the data compared have homogeneity of variance was

rejected. The Jarque-Bera test was used to assess the normality of the quantitative data (mean± SE). Normal and homogenous data were further analyzed using the Student's T-test or ANOVA followed by Tukey's *post hoc* test ($p< 0.05$). Non-homogenous data were analyzed with the Welch F test followed by Dunnett's *post hoc* test ($p< 0.05$). Non-parametric data were analyzed using the Kruskal-Wallis test and Dunn's *post hoc* test with Bonferroni correction ($p< 0.05$). Non-parametric Friedman's two-way ANOVA followed by Dunnett's *post hoc* test ($p< 0.05$) was performed to analyze miRNA concentration-dependent effects. All data is represented with the *post hoc* p-value for that data followed by the test p-value. The strength of correlation between AGO-binding miRNAs was calculated using the non-parametric Spearman's Rho (r_s) test, and the significance ($p< 0.05$) was determined using a 2-tailed test All statistical tests were performed using the PAST4 software (Hammer et al., 2001) and IBM SPSS statistics.

Chapter 3

Results

3. Results

3.1. Optimization of trophically delivered miRNA concentration

We first identified the dietary miRNA concentration leading to transcript downregulation and phenotypic changes in larval growth and development. A let-7 concentration-dependent decrease in the levels of target transcript *FTZ-F1* and *E74* was observed upon feeding an artificial diet supplemented with 4, 7, 10, 13, or 16 µg hairpin miRNA (pre-let-7) or mature miRNA (let-7). The *FTZ-F1* transcripts showed an 19-fold (p= 0.020) decrease upon the ingestion of 10 µg/g and higher pre-let-7concentrations, compared to the C larvae ($\chi^2_{(11)}$= 44.72, p< 0.0001) (Fig. 3a). On let-7, they showed a >41-fold (p= 0.002) decrease than C. *E74* transcript levels showed >23-fold (p= 0.04) reduction on the ≥10µg/g concentration pre-let-7 diets and >34-fold (p= 0.006) reduction on the ≥10µg/g concentrations let-7 diets than C ($\chi^2_{(11)}$= 43.68, p< 0.0001) (Fig. 3b).

This effect was also observed in larval growth and development. First instar duration gradually decreased from larvae that ingested 10 µg/g pre-let-7 diet (>1.3-fold, p= 0.004), >0.5-fold (p< 0.0001) on 13 µg/g diet, and >1.5-fold (p< 0.001) on 16 µg/g pre-let-7 diet ($\chi^2_{(11)}$ = 103.940, p< 0.001) (Fig. 3c). On the let-7-complemented diet, the first instar duration decreased ≥1.8-fold at 10, 13 and 16µg/g concentrations (p< 0.0001) than C. The first instar duration was ≥2.1-fold (p= 0.029) lower on the 10 µg/g let-7 diet than on the 10 µg/g pre-let-7 diet.

Pre-let-7 and let-7 diets showed similar effects on larval mass across the tested concentrations. Larval mass decreased ≥1.7-fold on the 10 µg/g (p< 0.001) pre-let-7 diet and ≥2.0-fold (p< 0.001) on the let-7 diet and remained constant at higher concentrations ($\chi^2_{(11)}$= 130.208, p< 0.001) (Fig. 3d). No difference was observed between the masses of pre-let-7 and let-7 -fed larvae across tested concentrations. Larval mortality was also similarly affected after pre-let-7 and let-7 feeding. At 10, 13 and 16 µg/g, it increased ≥1.8-fold (p= 0.014) on pre-let-7 diet and ≥1.9-fold (p= 0.016) on the let-7 diet ($\chi^2_{(11)}$= 37.499, p< 0.001) (Fig. 3e).

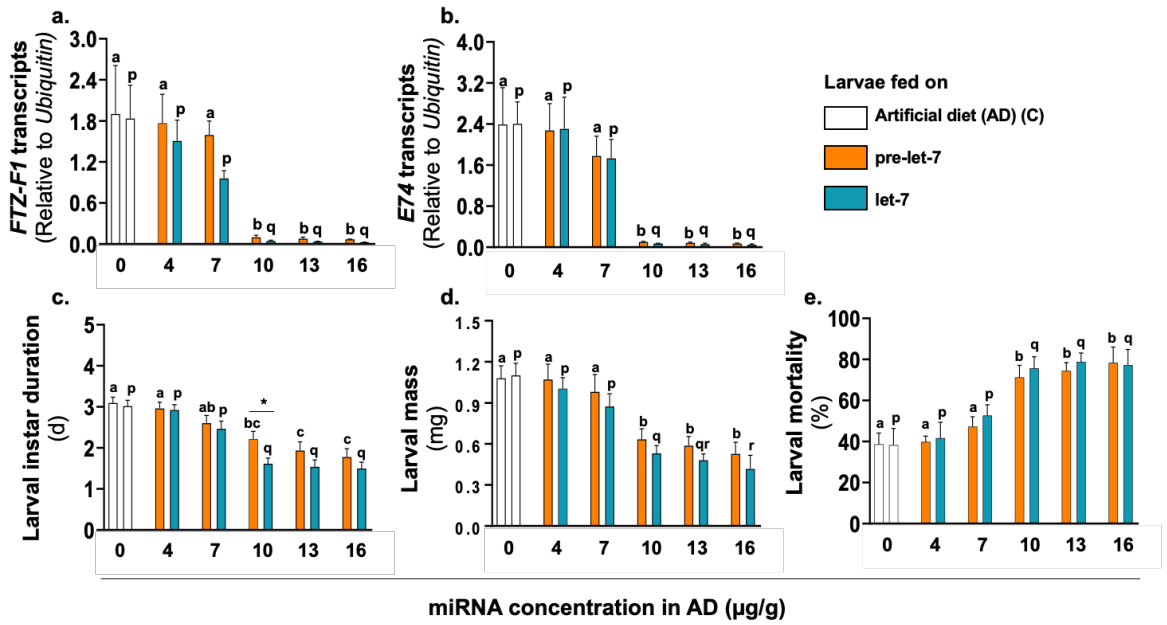

Figure 3 Validation of dietary miRNA's functionality in *P. xylostella* | a. *FTZ-F1* and **b.** *E74* transcript levels relative to *Ubiquitin* (20 pooled larvae, n= 5). **c.** Larval developmental time (mean ± SE, n= 30) from neonate to molting, **d.** larval mass (mg) (mean± SE, n= 30), and **e.** larval mortality after 24 h (%) (n= 5 sets, each containing 30 larvae). Significant differences were determined using Friedman's two-way ANOVA, and the statistical significance was determined using Dunn's *post hoc* test. Letters a, b, and c indicate significant differences between hairpin-fed larvae, letters p, q and r indicate significant differences between mature-fed larvae. Asterisk indicate significant difference between pre-let-7 and let-7-fed larvae.

3.2. let-7 ingestion increases let-7 levels and downregulates target transcripts

Pre-let-7 ingested larvae showed a ≥2.5-fold increase ($p \leq 0.04$) ($\chi^2 = 4.375$, $p = 0.01$) in the midgut pre-let-7 levels compared to the artificial diet (C) and let-7 ingested larvae (Fig. 4b). Let-7 levels increased 3.9-fold higher ($p = 0.024$) ($\chi^2 = 4.82$, $p = 0.006$) only on the let-7 diets compared to C and pre-let-7 larvae (Fig. 4c).

FTZ-F1 suppression was 11.8-fold ($p = 0.007$) ($\chi^2 = 17.41$, $p = 0.001$) after pre-let-7 and 15.1-fold ($p = 0.003$) after let-7 feeding compared to C (Fig. 4d). We observed a similar suppression after larvae were fed on pre-let-7-control (pre-C) and let-7-control (mature-C). *FTZ-F1* showed a 11-fold ($p < 0.001$) suppression after pre-let-7 feeding compared to pre-C and an 12.9-fold ($p = 0.007$) suppression after let-7 feeding compared to mature-C feeding. *E74* suppression was 13.9-fold ($p = 0.039$) ($\chi^2 = 18.26$, $p = 0.001$) on the pre-let-7 diet and 31.4-fold ($p = 0.003$) on the let-7 diet (Fig. 4e) compared to C. It showed a 14.5-fold ($p = 0.028$) suppression after pre-let-7 feeding compared to pre-C and a 41.3-fold ($p < 0.001$) suppression after let-7 feeding compared to mature-C feeding. There was no difference in transcript expression across C, pre-C, and mature-C-fed larvae.

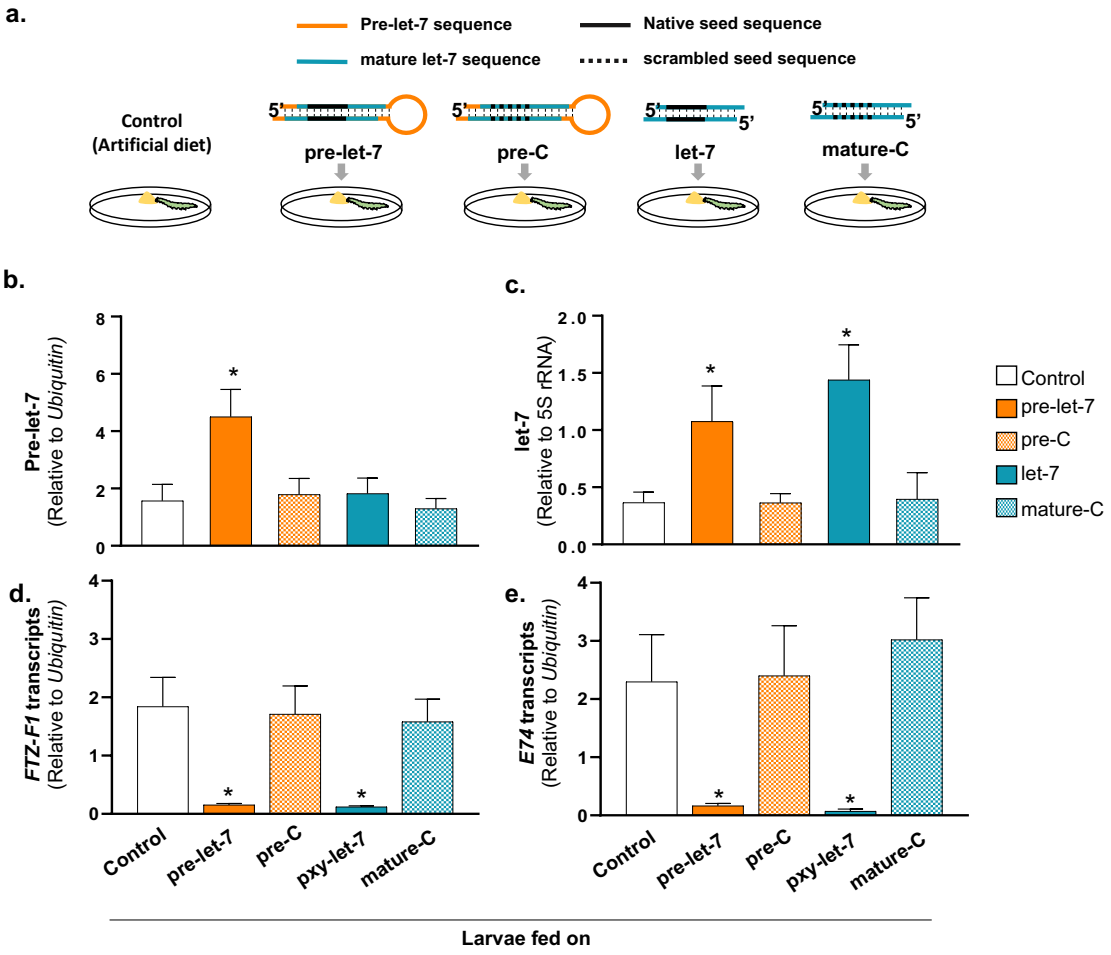

Figure 4 let-7 target expression after miRNA feeding | **a.** pre-let-7, **b.** let-7, **c.** *FTZ-F1* and ***d.*** *E74* expression levels (20 pooled larvae, n= 5). pre-let-7, *FTZ-F1,* and *E74* expression relative to *Ubiquitin*. Let-7 expression relative to 5S rRNA. Significant differences were determined by Kruskal-Wallis test followed by Dunn's *post hoc* test ($p \leq 0.05$). Asterisk denotes differences between treatments in every instar.

3.3. Effect of let-7 feeding on larval growth and development

Larvae showed a 1.3-fold reduction in larval durations on the pre-let-7 diet ($p< 0.001$) and 1.8-fold on the let-7 diet ($p< 0.0001$) than C ($F_{4,145}= 19.45$, $p< 0.0001$) (Fig. 5a). Larval duration reduced 1.4-fold ($p< 0.001$) on pre-let-7 compared to pre-C and 1.8-fold ($p< 0.0001$) on let-7 compared to let-7-C.

pre-let-7-fed and let-7-fed larvae consistently had lower mass than C-fed larvae. Larvae showed a 1.5-fold ($p= 0.002$) ($\chi^2= 54.39$, $p< 0.0001$) reduction in larval mass on the pre-let-7 diet than 2.1-fold ($p< 0.0001$) reduction on let-7 diet compared to C (Fig. 5b). No significant difference was observed between pre-let-7-fed and let-7-fed larvae. A decrease in larval mass after feeding on the pre-let-7 and let-7 diet compared to the pre-C or let-7 -C diet showed a similar trend to C diet-fed larvae. Larval mass was 0.5-fold ($p< 0.001$) reduced on pre-let-7 compared to pre-C and 2.4-fold ($p< 0.0001$) reduced on let-7 compared to let-7-C.

We also observed increased larval mortality in miRNA-fed larvae. On the pre-let-7 diet, mortality increased by 1.8-fold ($p< 0.001$) and by 1.9-fold ($p< 0.0001$) ($F_{4,20}= 18.45$, $p< 0.0001$) than the C-fed larvae (Fig. 5c).

Finally, larvae showed 1.9-fold ($p= 0.016$) and 2.2-fold ($p= 0.004$) decreased eclosion after feeding on the pre-let-7 and let-7 diet, respectively, than control ($F_{4,20}= 7.42$, $p< 0.001$). Although eclosion of larvae on pre-let-7 was similar to pre-C ($p= 0.053$), let-7-fed larvae eclosed 2.1-fold ($p= 0.011$) less than mature-C-fed larvae (Fig. 5d). Overall, hairpin and mature let-7 feeding affected growth and development in all larval instars.

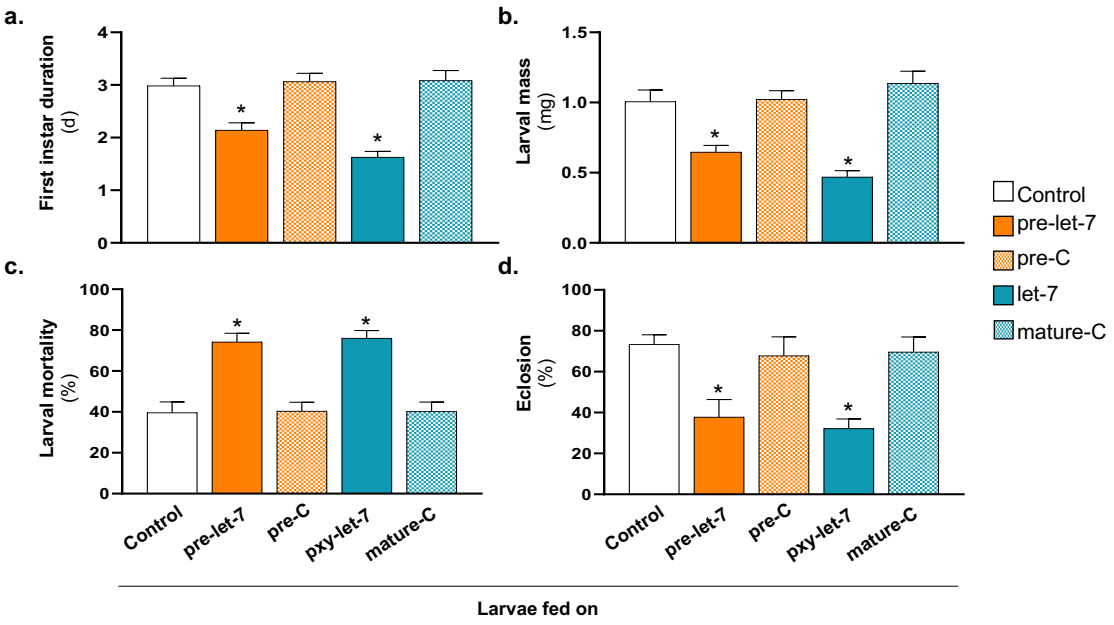

Figure 5 Larval and pupal developmental parameters after miRNA feeding. | a. Larval developmental time (mean± SE, n= 30), **b.** larval mass (mg) (mean± SE, n= 30), **c.** larval mortality after 24 h (%) (n= 5 sets, each containing 30 larvae), and **d.** eclosion (%) (n= 5 sets, each containing 100 pupae). For (**a**), (**c**) and **(d),** significance was calculated with one-way ANOVA followed by Tukey's *post hoc* test ($p \leq 0.05$). For (**b**), Kruskal-Wallis test was used followed by Dunn's *post hoc* test. Asterisk indicate significant difference between treatments.

3.4. Effect of *let-7* feeding on small RNA pathway components

Of the four sRNA pathway component transcripts analyzed, only Dicer-1 showed upregulation after pre-let-7 feeding (Fig. 6a). Larvae showed a 17.6-fold (p= 0.005) (χ^2= 11.79, p= 0.019) Dicer-1 upregulation than on C diet, respectively. Dicer-2 (Fig. 6b), AGO-1 (Fig. 6c), and AGO-2 (Fig. 6d) did not show any effect between treatments.

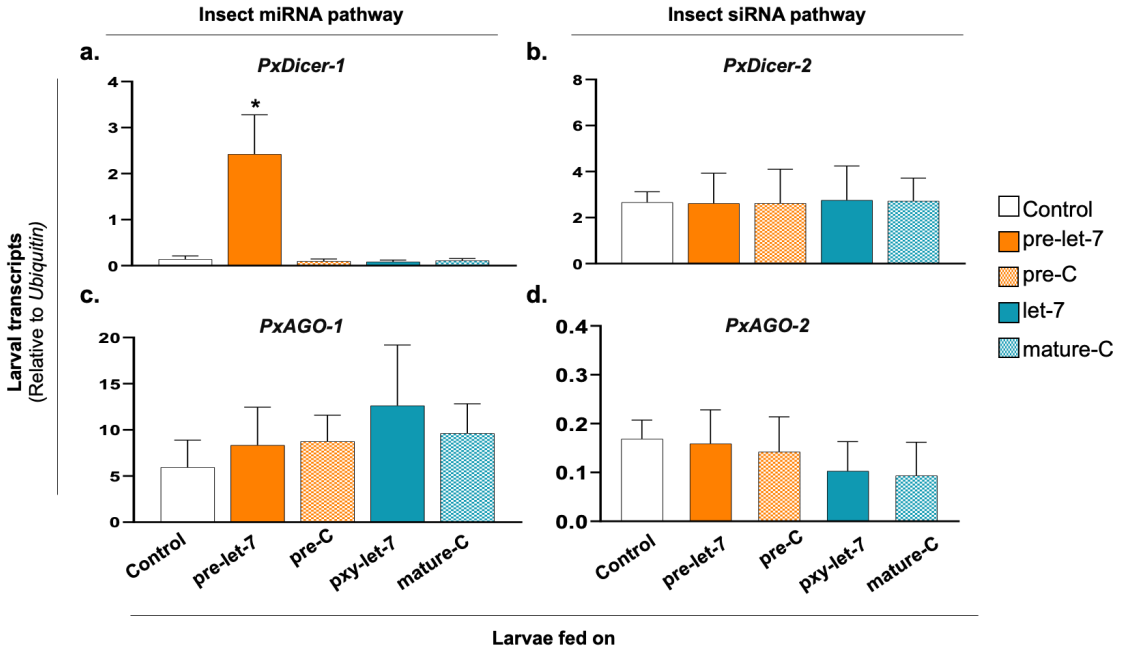

Figure 6 Effects of miRNA feeding on miRNA and siRNA pathway components. | Transcript levels (relative to *Ubiquitin*) of **a.** *Dicer-1*, **b**. *Dicer-2*, **c.** *AGO*-1, and **d.** *AGO-2*. Significance was determined by Kruskal-Wallis test followed by Dunn's *post hoc* test ($p \leq 0.05$). Asterisk indicate significant difference between treatments.

3.5. *A. thaliana* miRNA putatively targets *P. xylostella* genes

2 (1.56%), 81 (63.28%), and 45 (35.15%) identical miRNA-target pairs were obtained for 5' UTR, CDS, and 3' UTR, respectively, across three algorithms (Fig. 7a). A total of 56 unique miRNAs putatively targetting *P. xylostella* transcripts were identified.

The analysis revealed that cellular metabolic processes (12.1%) and organic substance metabolic processes (11.2%) were the major biological process groups. In terms of molecular function, hydrolase activity (18.7%) was the most represented category, including various genes such as glucosinolate sulfatase, carboxylpeptidase B-like, serine/threonine-protein phosphatase 5, among others (Fig. 7b).

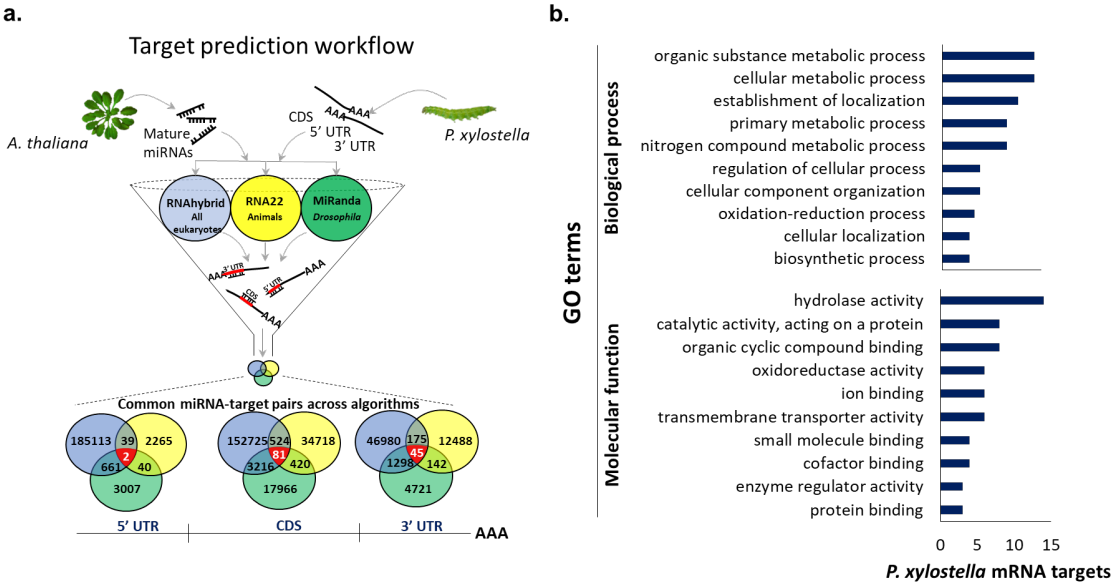

Figure 7 *A. thaliana* miRNA target prediction in *P. xylostella* midgut transcriptome | **a**. Target prediction algorithms, viz.- RNAhybrid (used for all eukaryotes), RNA22 (animal-specific algorithm) and MiRanda (*D. melanogaster*-specific algorithm) were used for predicting *A. thaliana* miRNA targets in *P. xylostella* midgut transcriptome. Venn diagrams depict the number of common miRNA-mRNA target pairs across algorithms for 5' UTR, CDS, and 3'UTR. **b.** Gene ontology graphs for "Biological process" and "Molecular function" for all putative *P. xylostella* target mRNAs

3.6. Assessing miRNA compatibility with *P. xylostella* miRNA machinery

To test compatibility between *A. thaliana* miRNAs and *P. xylostella* miRNA machinery, we hypothesized two scenarios- first, *A. thaliana* pre-miRNAs are amenable to processing by *P. xylostella* Dicer-1 (Fig. 8a), and second, *A. thaliana* mature miRNA duplexes are compatible with processing by *P. xylostella* AGO-1 or AGO-2 (Fig. 8b). For this, we performed sequence and structural comparisons of the sRNA protein

components in *A. thaliana* and *P. xylostella.*

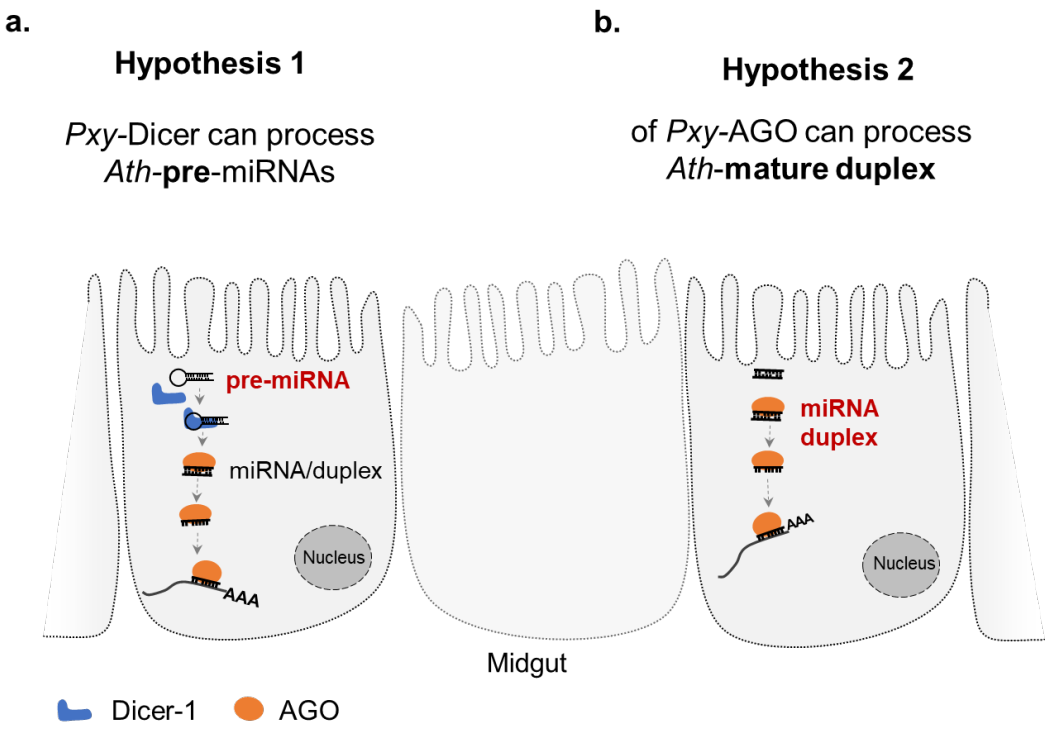

Figure 8 Fate of plant-origin miRNAs in insect | **a**. Hypothesis 1: *A thaliana* pre-miRNAs are amenable to processing by *P. xylostella* Dicer-1. **b**. Hypothesis 2: *A. thaliana* mature miRNA duplex is amenable to processing by *P. xylostella* AGO.

3.7. Dicer phylogeny

The fate of *A. thaliana* pre-miRNA entering the insect cell would be determined by its compatibility with *P. xylostella* Dicer proteins (Fig 8a). The phylogenetic tree showed two distinct Dicer-1 and Dicer-2 clades (Fig. 9b). It also revealed the independent clades of Animal Dicer and Dicer-like proteins (DCL) from plants in consensus with previous findings (Mukherjee et al., 2013). Putative Dicer proteins from *P. xylostella* separated in independent clades; XP_037972432.1 Endoribonuclease Dcr-1-like being part of the Dicer-1 clade. Similar to *D. melanogaster* Dicer-1 (the positive control), the putative *P. xylostella* Dicer-1 sequence showed the presence of all characteristic domains, viz. dBF, Dimer, PBD, DSRM, RNAseIIIa, RNAseIIIb, PAZ, and DEXDc (Paturi & Deshmukh, 2021) (Fig. 9a). We confirmed the absence of the 'DECH' (Walker-B motif) in XP_037972432.1 (NCBI), which is a Dicer-1 character (Tsutsumi et al., 2010) (Fig. 9c). The other protein (XP_037969486.1 (NCBI)) showed conservation of the 'DECH' motif in the DEAD-like helicase domain, similar to insect Dicer-2.

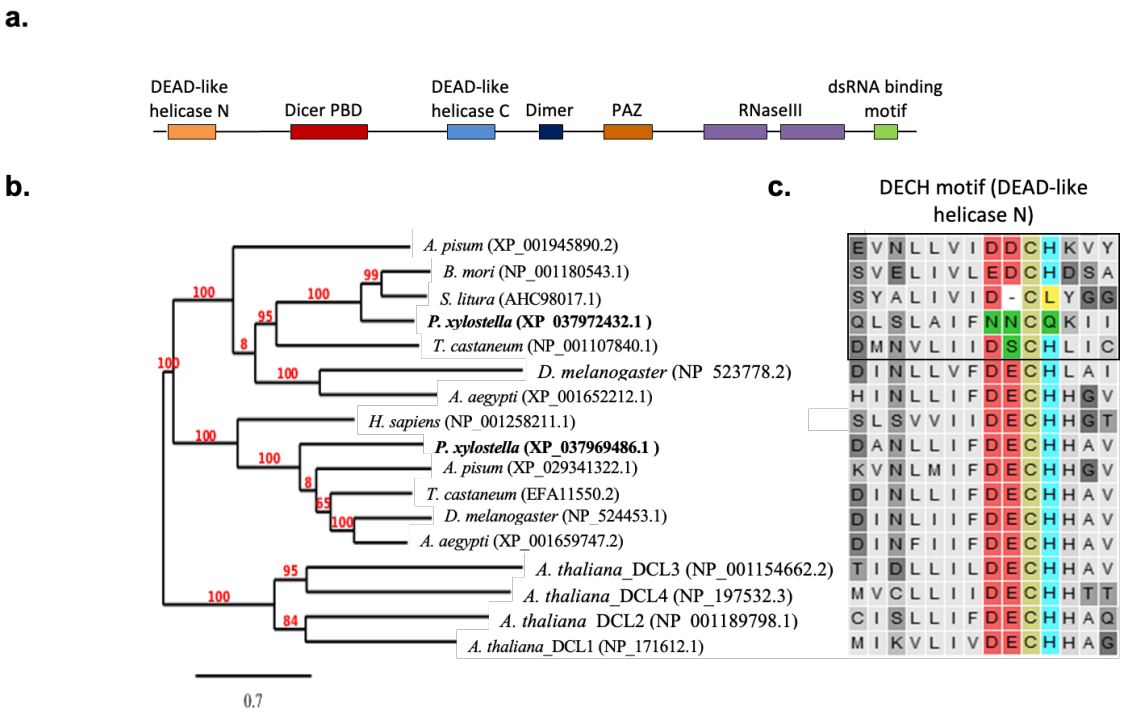

Figure 9 *P. xylostella* Dicer-1 annotation | **a**. Representation of canonical domains of Dicer-1. **b**. Phylogenetic analysis using the maximum likelihood method (rendered on Phylogeny.fr). Values at nodes represent branch support values (%). **c**. multiple sequence alignment of respective protein sequences from the phylogenetic tree. Box denotes sequences not showing the DECH motif.

3.8. Comparison of Dicer domains

Pxy-Dicer-1 DEAD-like Helicase N, Dicer PBD, DEAD-like Helicase C, Dimer, PAZ, RNAseIIIa, RNAseIIIa, and dsRNA binding motifs were 26%, 41%, 49%, 54%, 64%, 58%, 45%, and 81% similar to their respective *Dme*-Dicer-1 domains, respectively. We superimposed homology-based modeled domains to determine the structural similarity between *Pxy*-Dicer-1 and *Dme*-Dicer-1. Superimposition from SWISS-MODEL, Modweb, and Phyre2.0 yielded RMSDs of 1.2 Å (DEAD-like helicase N), 0.401 Å (Dicer PBD), 0.816 Å (DEAD-like helicase C), 1.11 Å (Dimer), 0.914 Å (PAZ), 1.192 Å (RNAseIIIa), 0.593 Å (RNAseIIIb), and 1.166 Å (dsRNA binding motif) (Fig. 10a-h). Between *P. xylostella* Dicer-1 and *A. thaliana* DCL-1, the Helicase C-terminal domain (Fig. 10j) showed a lower (0.750 Å) RMSD (hence higher overlap) than PAZ (1.403 Å) (Fig. 10i).

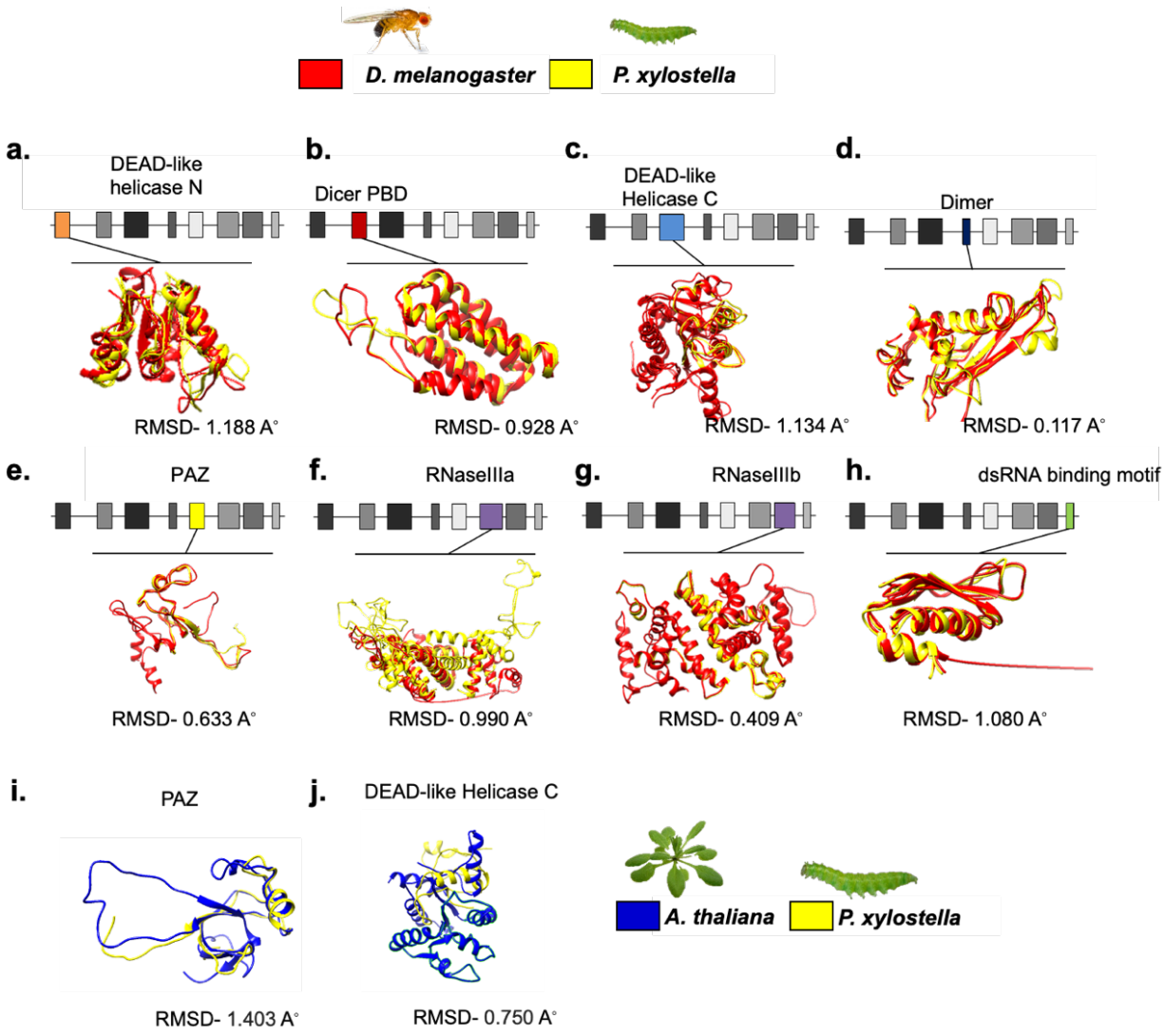

.

Figure 10 Structural conservation of the Dicer domains | a-h. Comparison of *D. melanogaster* (red) and *P. xylostella* (yellow) domain structures. Colored boxes above structures denote the location of the domain along the protein. **i-j.** Domain overlap between *A. thaliana* (blue) and *P. xylostella* (yellow) PAZ (function to measure stem length of pre-miRNA) and Helicase C-terminal domain (function to determine loop length of pre-miRNA).

3.9. Structural features of pre-miRNA

CP-pre and nCP-pre were ≥2.9-fold longer than both insect species ($p< 0.0001$) ($\chi^2= 280.7$, $p< 0.0001$) (Fig. 11a). There was no difference in *Dme*-pre and *Pxy*-pre. Though *A. thaliana* pre-miRNAs have longer stem lengths, 99.93% CP-pre and 82.18% nCP-pre miRNA stem lengths were in the *Pxy*-pre stem range. The 5- stems of CP-pre and nCP-pre were 1.4- and 1.7-fold longer than the insects' ($p< 0.0001$) ($\chi^2= 187.2$, $p< 0.0001$), respectively (Fig. 11b). The 3- stems of filtered CP-pre and nCP-pre were 0.5- and 1.7-fold longer than the insects' ($p< 0.0001$) ($\chi^2= 180.6$, $p< 0.0001$), respectively (Fig. 11c). CP-pre loop lengths were in the *Pxy*-pre loop range, while nCP-pre loops were 1.2-fold longer than *Dme*-pre ($p< 0.001$) ($\chi^2= 13.46$, $p= 0.003$) (Fig. 11d). Overall, 98.04% loop lengths, 86.34% 5p-stem, and 89.26% 3p-stem lengths of nCP-pre overlapped with the insect range (Fig. 11b-d).

CP-pre 5p-dicing sites were significantly different from *Dme*-pre ($p= 0.001$) ($\chi^2= 32.38$, $p< 0.001$) (Fig. 11e) but CP-pre 3p-dicing sites did not differ from *Dme*-pre 3p-dicing sites ($\chi^2= 17.81$, $p< 0.001$) (Fig. 11f). Dicing sites between *Pxy*-pre and *Dme*-pre and CP-pre and nCP-pre, respectively, were comparable for both 5p and 3p dicing sites. nCP-pre was significantly different than *Dme*-pre ($p< 0.0001$ for 5p & $p< 0.01$ for 3p start site). There was no significant difference in the distribution of dicing sites in CP-pre and *Pxy*-pre for 5p and 3p start sites.

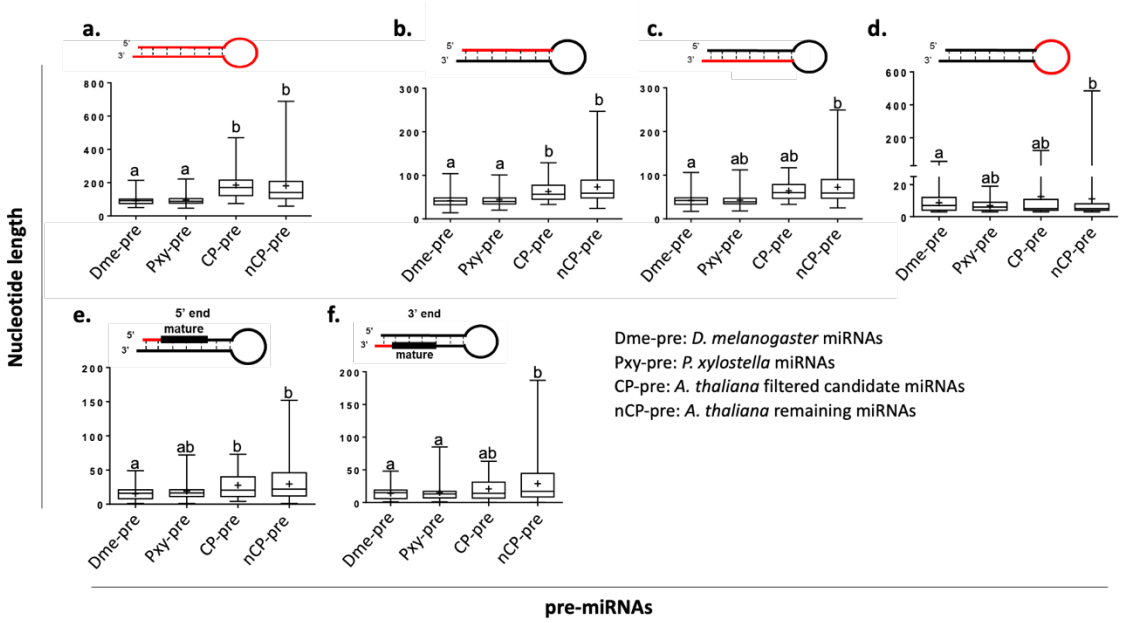

Figure 11 Features of pre-miRNAs | Pre-miRNA features from *P. xylostella* (n= 30) comparing *D. melanogaster* (n= 30), CP (n= 51), and nCP (n= 65). Red denotes the pre-miRNA feature [nucleotide length (no. of bases)]) for **a.** Pre-miRNA length **b.** 5p stem length, **c.** 3p stem length, **d.** loop length **e.** 5p mature miRNA start site (dicing site) and **f.** 3p mature miRNA start site (dicing site). Significant differences ($p \leq 0.05$) were determined by the Kruskal-Wallis test, followed by Dunn's *post hoc* test.

3.10. Phylogenetics and structural analysis of Argonaute proteins

Out of the five putative *Pxy*-AGO and AGO-like proteins, two clustered in the AGO-2 clade and one each in the AGO-1, AGO-3, and AUB/PIWI domain-containing protein clades (Fig. 12a). Distinct clades of AGO-1, AGO-2 & AGO-3 were observed in the phylogenetic tree, Plant AGOs and the insect AGO-1 clade shared a common ancestor, which together shared a common ancestor with the insect AGO-2 clade.

High overlap was observed between AGO-1 (RMSD= 0.169 Å) (Fig. 12b) and AGO-2 (RMSD= 0.791 Å) (Fig. 12c) of both insect species. The overlap between *Pxy*-AGO-1 and *ath*-AGO-1 (RMSD= 1.072 Å) was lower than between insects (Fig. 12d).

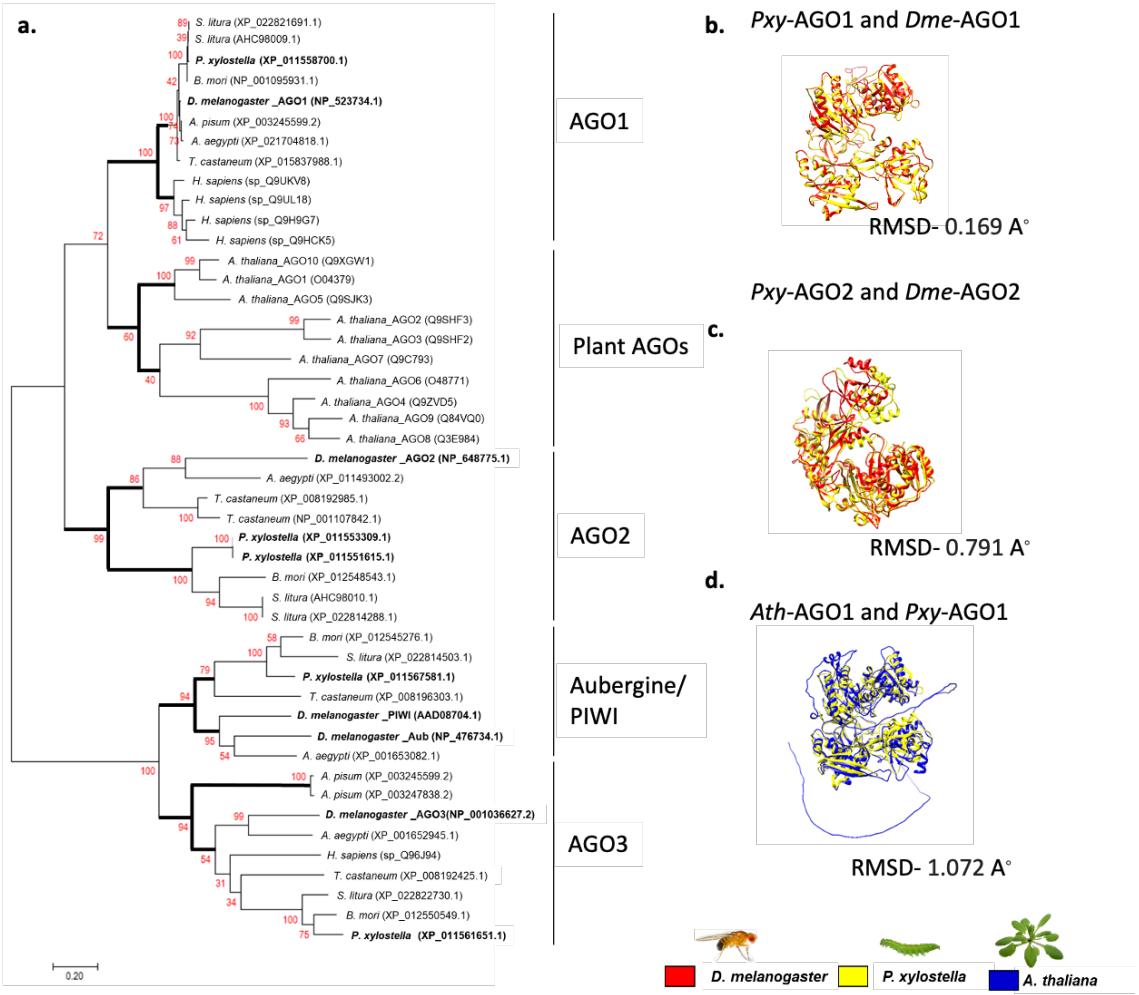

Figure 12 AGO phylogenetic and structural analysis | a. Phylogenetic analysis using maximum likelihood with a bootstrap value of 1000 showing different clustering of AGO and AGO-like proteins in animals and plants (rendered on Phylogeny.fr). Values at nodes represent branch support values (%). Structural superimposition between **b**. *pxy*-AGO-1 and *dme*-AGO-1, **c**. *pxy*-AGO-2 and *dme*-AGO-2, and **d**. *ath*-AGO-1 and *pxy*-AGO-1. Overlaps were constructed using Chimera 1.15.

3.11. Uptake and loading of foreign miRNAs on *P. xylostella* Argonaute protein

We observed a positive correlation between miRNA groups, except in *Dme*-AGO-2-md *compared* to CP-md and nCP-md (Fig. 13b). A more robust correlation was observed between *Dme*-AGO-1-md and *Pxy*-md (rs= 0.99, $p< 0.0001$) compared to the correlation between *Dme*-AGO-2-md and *Pxy*-md (rs= 0.65, $p= 0.038$). CP-md did not correlate with *Dme*-AGO2-md and positively correlated with *Dme*-AGO-1-md (rs= 0.70, $p= 0.021$) and *Pxy*-md (rs= 0.78, $p= 0.007$).

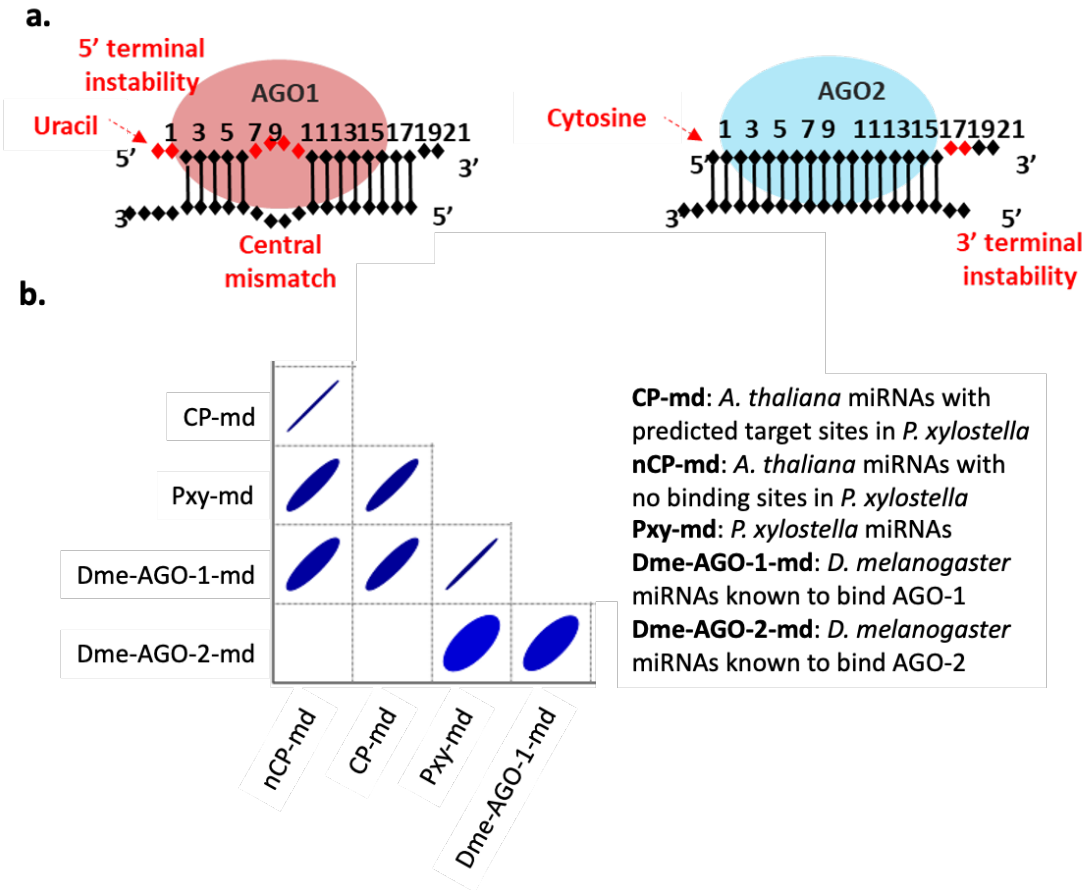

Figure 13 AGO sorting characters of filtered *A. thaliana* miRNAs | a. Criteria used for sorting the duplexes: (1) identity of the first nucleotide of miRNA's 5' end: if uracil (U), then duplex is sorted as AGO-1-loading and if cytosine (C), the duplex is sorted as AGO-2-loading, a mismatch at the terminal end of the duplex, (2) duplexes with unpaired 5' end were sorted as AGO-1 loading, and those with unpaired 3' end as AGO-2 loading, and (3) Central mismatch at positions spanning 8-11 nucleotide from 5' end; duplexes with a mismatch in the central region were sorted as AGO-1 loading and those with no mismatch as AGO-2 loading. **b.** Spearman's correlation between 5' sorting parameters.

3.12. miRNAs putatively targeting insect transcripts are induced upon herbivory

10 miRNAs showed upregulation after 1 h herbivory (Hb) and wounding + oral secretion (W+OS) compared to wounding + water (W+W) and no treatment (NT) . *ath*-miR396 >5-fold (χ^2= 14.28, p= 0.001) (Fig. 14d), *ath*-miR398a >20-fold (χ^2= 16.72, p< 0.001) (Fig. 14e), *ath*-miR5023 >23-fold (χ^2= 16.58, p< 0.001) (Fig. 14k), *ath*-miR5634 >4fold (χ^2= 17.3, p< 0.001) (Fig. 14n), *ath*-miR5661 >12-fold (χ^2= 11.13, p= 0.011) (Fig. 14m), *ath*-miR8165 >4-fold (χ^2= 15.17, p= 0.001) (Fig. 14o), *ath*-miR8168 >9-fold (χ^2= 13.87, p= 0.003) (Fig. 14p), *ath*-miR8171 >990-fold (χ^2= 15.42, p= 0.001) (Fig. 14q), *ath*-miR8173 >11-fold (χ^2= 16.2, p= 0.001) (Fig. 14r), and *ath*-miR8180 showed a >17-fold (χ^2= 14.78, p= 0.002) (Fig. 14t) upregulation on the Hb and W+OS treatments as compared to NT and W+W controls after 1 h. *ath*-miR2934 showed >6-fold (χ^2= 14.22, p= 0.002) (Fig. 14j), *ath*-miR169 >19-fold (χ^2= 11.11, p= 0.011) (Fig. 14c), and *ath*-miR414 >17-fold (χ^2= 12.25, p= 0.006) (Fig. 14g) upregulation on the Hb and W+OS compared to NT, but not W+W. miR165 (~3-26-fold) (Fig. 14b) showed a maintained induction for up to 72 h (χ^2= 18.95, p< 0.001). *ath*-miR5660 (Fig. 14l) and *ath*-miR8176 (Fig. 14s) did not show any response to herbivory.

ath-miR164, *ath*-miR447, and *ath*-miR824, miRNAs that putatively target *GSS1* and *GSS2* (Fig. 15a), the glucosinolate sulfatase transcripts (Fig. 15e), showed induction after herbivory. *ath*-miR164 showed a maintained induction up to 72 h on Hb and W+OS compared to W+W and NT (Fig. 15b). Induction at 1 h was >6-fold ($p\leq$ 0.038) (χ^2= 12.13, p= 0.006), >3-fold ($p\leq$ 0.030) (χ^2= 14.7, p= 0.002) at 3 h, >4-fold ($p\leq$ 0.024) (χ^2= 12.5, p= 0.005) at 24 h, >3-fold ($p\leq$ 0.002) (χ^2= 17.21, p< 0.001) at 48 h, and >5-fold ($p\leq$ 0.009) (χ^2= 14.616, p= 0.002) at 72 h. *ath*-miR447 induced 90.3-fold (p< 0.0001) (χ^2= 16.8, p< 0.001) compared to WT (Fig. 15c). *ath*-miR824 upregulated >8-fold ($p\leq$ 0.020) (χ^2= 14.61, p= 0.002) 1 h on Hb compared to W+W and NT and >4-fold ($p\leq$ 0.009) (χ^2= 15.82, p= 0.001) after 48 h on Hb and W+OS compared to W+W and NT (Fig. 15d).

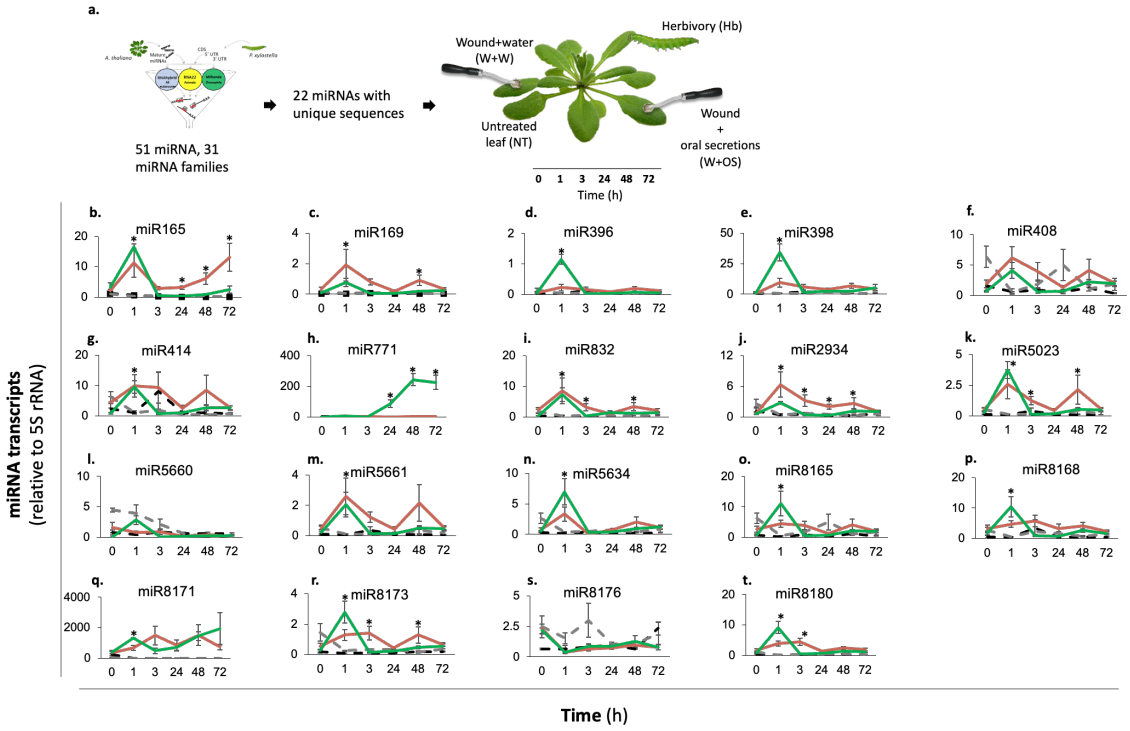

Figure 14 Effects of herbivory on miRNA expression | a. Schematic of the time-course miRNA induction assay. **b-t.** miRNA transcript abundance (relative to 5S rRNA) in treated and control leaves (n= 6 biological replicates). Asterisks denote significant differences ($p \leq 0.05$) determined using Kruskal-Wallis test followed by Dunn's *post hoc* test.

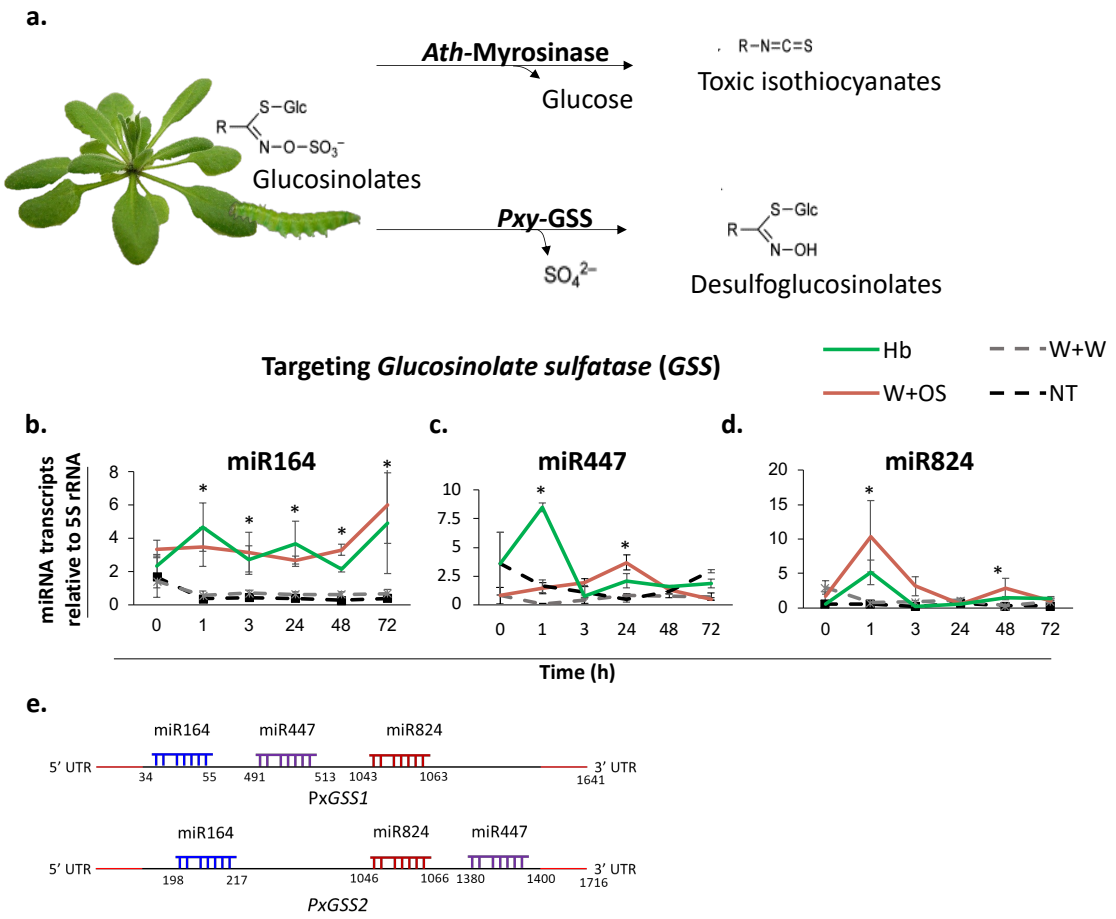

Figure 15 Induction of putative *glucosinolate sulfatase* targeting miRNAs | a. Schematic of the glucosinolate-myrosinase system in *A. thaliana*. and Glucosinolate sulfatase (GSS)-mediated counter-defense. Transcript levels of **b.** *ath*-miR164 **c.** *ath*-miR447**, d.** *ath*-miR824 that putatively target (relative to 5S rRNA). Asterisks denote significant differences ($p \leq 0.05$) determined using Kruskal-Wallis and Dunn's *post hoc* test. **e.** Schematic of binding sites of *ath*-miR164, *ath*-miR447, and *ath*-miR824 on *GSS1* and *GSS2.* Numbers below the target site denote nucleotide binding location.

3.13. Dietary uptake of *ath*-miR164, *ath*-miR447 and *ath*-miR824 miRNAs reduces *GSS* expression

Ingestion of *ath*-miR164, *ath*-miR447, and *ath*-miR824 complemented on leaves (L+miR) (Fig. 16a) reduced *GSS1* levels after 24 h compared to leaf + water (L+W). The *ath*-miR824-fed reduction was the strongest (10.2-fold) ($t_{(6)}$= 3.26, p= 0.008) (Fig. 16d), followed by *ath*-miR164 (5.9-fold) ($t_{(6)}$= 2.99, p= 0.013) (Fig. 16b), and *ath*-miR447 (4.9-fold) ($t_{(6)}$= 2.80, p= 0.018) (Fig. 16c) than L+W. In *ath*-miR164, reduction persisted in 48 h (4.9-fold) ($t_{(6)}$= 4.39, p= 0.002) and 72 h (13.5-fold) ($t_{(6)}$= 5.73, p= 0.004) in L+miR compared to L+W (Fig. 16b). *GSS2* levels were also found to be reduced upon miRNA feeding at 24 h. They reduced (2.4-fold) ($t_{(4)}$= 3.39, p= 0.011) after *ath*-miR164 (Fig. 16e), 3.8-fold) ($t_{(4)}$= 6.15, p< 0.001) after *ath*-miR447 (Fig. 16f) and (3.3-fold) ($t_{(4)}$= 4.39, p= 0.004) (Fig. 16g) after *ath*-miR824, compared to L+W. No miRNAs showed *GSS2* repression beyond that.

Pxy-miR375, *Pxy*-miR8534, and *Pxy*-miR8533 feeding showed decreased *CYP4G15* (6.6-fold) ($t_{(6)}$= 2.65, p= 0.026) (Fig. 17a), *CYP6B6* (6.1-fold) ($t_{(6)}$= 2.68, p= 0.022) (Fig. 17c), and *LCP30* levels (16.8-fold) ($t_{(6)}$= 2.65, p= 0.024) (Fig. 17e) at least up to 48 h compared to L+W, respectively. To confirm that *ath*-miR164, *ath*-miR824, and *ath*-miR447 do not show off-target effects, we the mRNA levels after feeding these *ath*-miRNA. No change in *CYP4G15* (Fig. 17b), *CYP6B6* (Fig. 17d), and *LCP30* (Fig. 17f) levels was observed after feeding *ath*-miR164, *ath*-miR824, and *ath*-miR447 in L+miR compared to L+W.

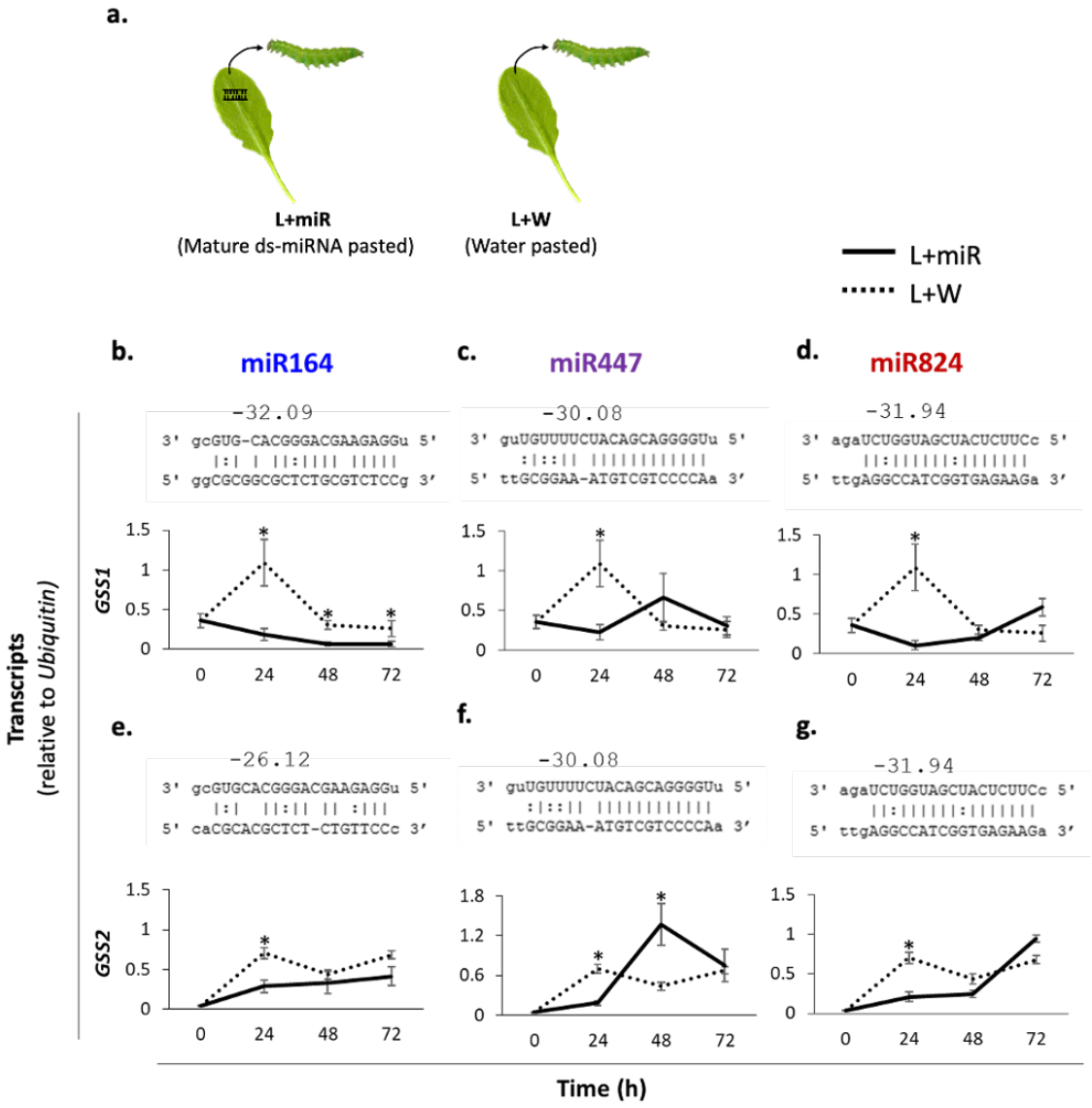

Figure 16 Effect of miRNA ingestion on *GSS* levels | a. Schematic of miRNA-feeding assay. 10 µg mature miRNA duplexes (*ath*-miR164, *ath*-miR447, and *ath*-miR824) were complemented on WT *A. thaliana* leaves and larvae were dissected to harvest midgut tissue. Transcript abundance of *GSS1* after **b.** *ath*-miR164, **c.** *ath*-miR447, and **d.** *ath*-miR824 ingestion; and *GSS2* after **e.** *ath*-miR164, **f.** *ath*-miR447, and **g.** *ath*-miR824 (c.) relative to *Ubiquitin*. Significant differences (* ≡ $P \leq 0.05$) were determined by Student's t-test (2-tailed). Nucleotide interactions above graphs represent miRNA binding to *GSS* with the number denoting free energy change of binding (ΔG).

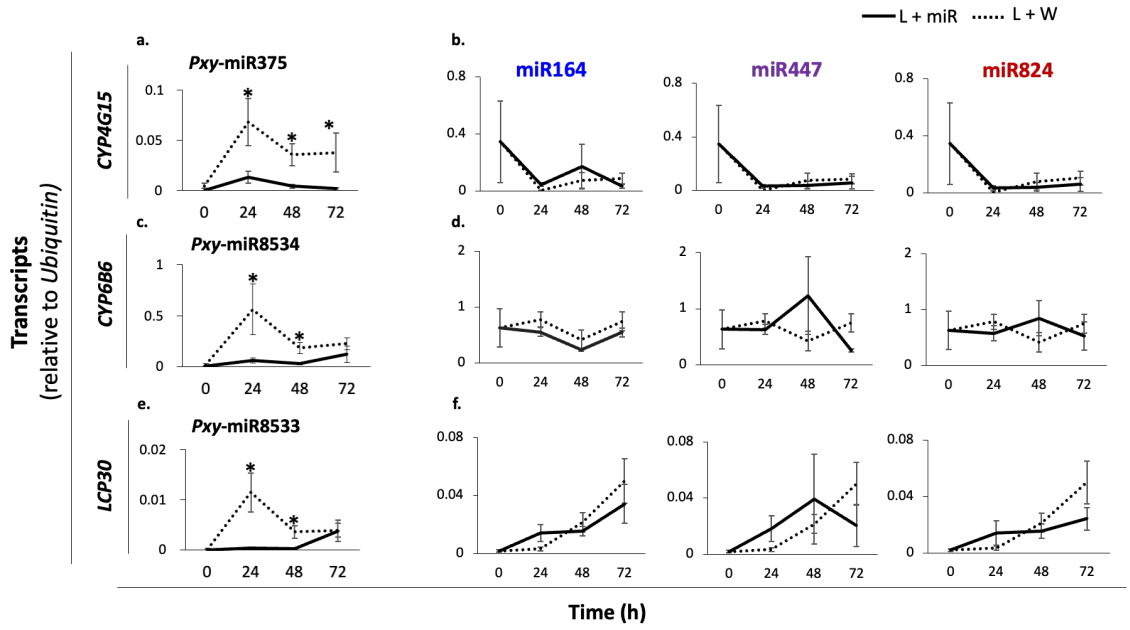

Figure 17 Confirmation of GSS-specific effects of *ath*-miRNA ingestion | Transcript levels of **a.** *CYP4G15*, **c.** *CYP6B6*, and **e.** *LCP30* after *Pxy*-miR375, *Pxy*-miR8534 and *Pxy*-miR8533 ingestion, respectively (Relative to *Ubiquitin*). Effect of *ath*-miR164, *ath*-miR447, and *ath*-miR824 on **b.** *CYP4G15*, **d.** *CYP6B6*, and **f.** *LCP30* transcript levels. Significant differences (* ≡ $p \leq 0.05$) were determined by Student's t-test (2-tailed).

3.14. *Ath*-miR164 feeding affects *P. xylostella* larval performance

After ingesting RNA-complemented (*ath*-miR164, *ath*-pre-miR164, and ds*GSS1*) WT plants, larval mass was 2.8-3.2-fold lower than untreated ($p< 0.001$) and water-complemented ($p< 0.001$) WT plants and 3.1-3.5-fold lower than control ($p\leq 0.00001$) or RNA-complemented *myb28myb29*-fed plants ($p\leq 0.001$) ($\chi^2= 124$, $p< 0.001$) (Fig. 18b). The first instar duration on larvae fed on RNA-complemented WT plants was >2.6-fold than the WT controls ($p\leq 0.0001$) (Fig. 18c). This duration also increased 2.8-3-fold more than *myb28myb29*-fed larvae ($p< 0.0001$) (F= 37.58, df= 117.6, $p< 0.0001$). Along with growth parameters, larval mortality increased ≥3.2-fold compared to WT controls ($p\leq 0.001$) and ≥6.1-fold compared to larvae fed on *myb28myb29* plants ($p\leq 0.0001$) ($F_{9,40} = 27.86$, $p< 0.001$) (Fig. 18d). There was no difference in mortality in larvae feeding on control *myb28myb29* plants and RNA-complemented *myb28myb29* plants. (Fig. 19a). Glucoraphanin (Fig. 19b) and desulfoglucoraphanin (Fig. 19c) reduced 3.1-3.5-fold ($p\leq 0.05$) ($F_{4,25}= 9.154$, $p< 0.001$) and 6.9-9.9-fold ($p\leq 0.05$) (F= 18.92, df= 11.63, $p< 0.0001$) in RNA-fed larvae compared to untreated and water-complemented controls, respectively. The isothiocyanate form, sulforaphane (Fig. 19d), increased 455-5.6-fold ($p\leq 0.05$) (F= 11.89, df= 11.61, $p< 0.0001$) in these larvae compared to controls.

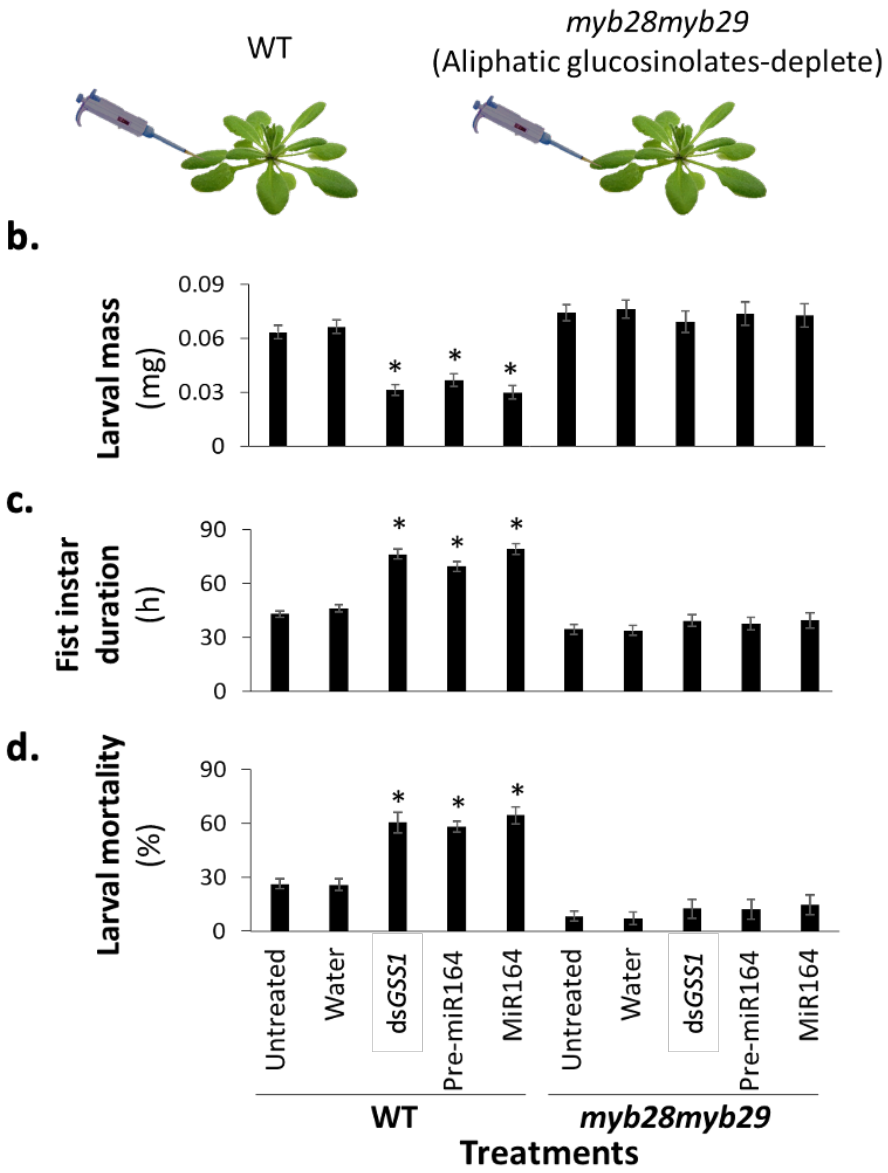

Figure 18 ***ath*-miR164's dietary uptake affects larval performance | a.** *ath*-miR164, *ath*-pre-miR164, and *GSS1*-specific dsRNAs were complemented on WT or *myb28myb29* leaves **b.** Larval mass (mg) (mean ± SE, n= 30), c. larval developmental time (h) (mean ± SE, n= 30) from neonate to molting, and d. larval mortality after 24 h (%) (n= 6 sets, each containing 30 larvae). Significant differences for (**b**) were determined using Kruskal-Wallis test, followed by Dunn's *post hoc* test ($p \leq 0.05$). Significance for (**c**) was determined by Welch's F test followed by Dunnett's *post hoc* test ($p \leq 0.05$). Significance for (**d**) was determined using Fisher's one-way ANOVA, followed by Tukey's *post hoc* test ($p \leq 0.05$). Asterisk indicates a significant difference between treatments.

.

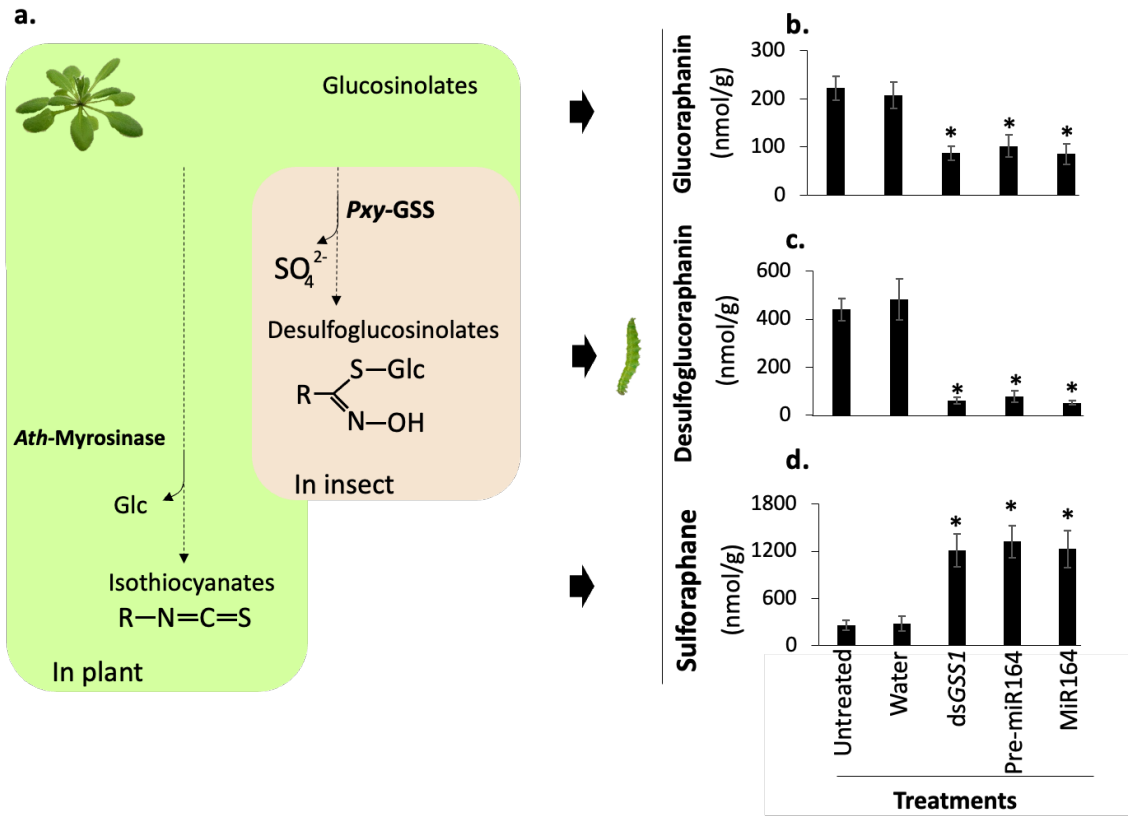

Figure 19 *ath*-miR164 feeding affects glucosinolate metabolism | a. Schematic of the glucosinolate-myrosinase system. **b-d.** Metabolite concentration measured (nmol/g) after *P. xylostella* feeding on control or RNA-complemented WT leaves: **b.** Glucoraphanin, **c.** desulfoglucoraphanin, and **d.** sulforaphananane. Significant differences between mean ± SE in (**b**) were analyzed by one-way ANOVA followed by Tukey's *post hoc* test ($p \leq 0.05$). Significant differences between mean ± SE in (**c**) and (**d**) were analyzed by Welch's F test, followed by Dunnett's *post hoc* test ($p \leq 0.05$). The asterisk indicates a significant difference between treatments.

3.15. *Ath*-miR164-mediated effects affect *P. xylostella*'s parasitoid but not the predator

D. semiclausum showed no ovipositioning preference towards RNA-fed (ds*GSS1*, pre-miR164, miR164-complemented) or control (untreated or water-complemented) larvae, irrespective of feeding on WT- or *myb28myb29*-complemented leaves. This was true for both choice ($F_{9,40}$= 0.1278, p= 0.998) (Fig. 20c) and no-choice ($F_{9,40}$= 0.3079, p= 0.967) assays (Fig. 20b), suggesting no preference towards RNA-fed or unfed larvae. A 8.7-9.5-fold (p< 0.04) ($F_{9,40}$= 16.76, p< 0.001) increase in mortality was observed in wasps oviposited in RNA-fed larvae on WT leaves compared to WT controls or on RNA-fed larvae on *myb28myb29* leaves (Fig. 20d).

The predation choice ($F_{9,40}$= 0.1675, p= 0.996) (Fig. 20f) and no-choice assays ($F_{9,40}$= 0.1733, p= 0.995) (Fig. 20e) for *C. carnea* showed no preference towards any *P. xylostella* larvae. There was negligible *C. carnea* larval mortality between treatments, and no difference was observed between *C. carnea* fed on RNA-fed or control-fed *P. xylostella* (F= 0.3175, df= 20.63, p= 0.959) (Fig. 20g).

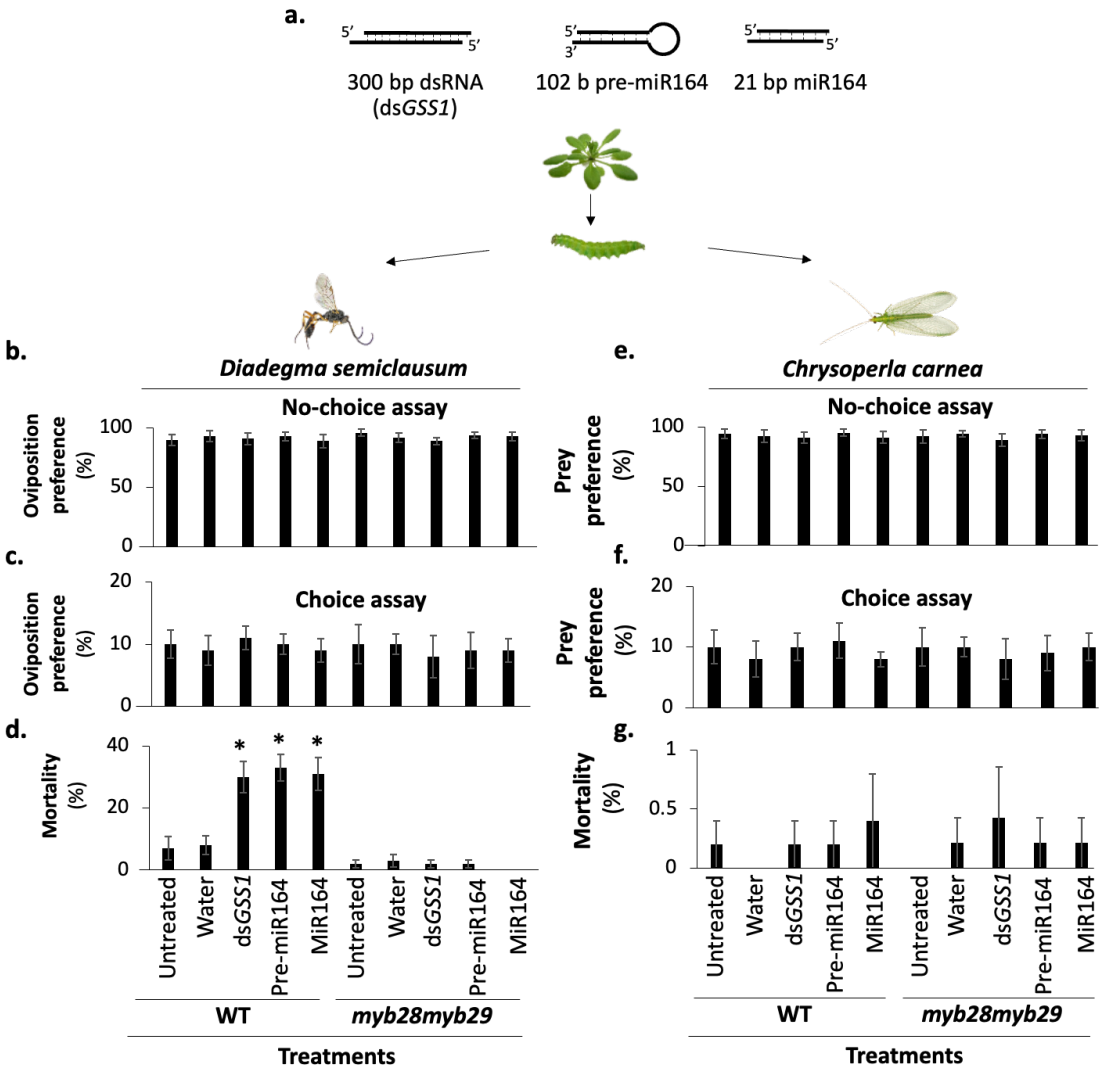

Figure 20 Effect of *ath*-miR164 feeding on *P. xylostella*'s natural enemies | a. schematic of assay setup. *P. xylostella* larvae fed on different conditions were provided to the natural enemies. (**b-d**) *D. semiclausum* was allowed to oviposit on *P. xylostella* larvae fed on different treatments. **b.** Ovipositioning events (%) in a no-choice setup (mean ± SE). **c.** Ovipositioning events (%) in a choice assay setup (mean ± SE). **d.** Mortality (%) after development in *P. xylostella* larvae (mean ± SE). (**e-g**) *C. carnea* was allowed to predate on *P. xylostella* larvae fed on different treatments. **e.** Predation (%) in a no-choice setup (mean ± SE). **f.** Predation (%) in a choice setup (mean ± SE). **g.** Mortality (%) after predation (mean ± SE). Significance for (**d**) was determined using Fisher's one-way ANOVA followed by Tukey's *post hoc* test ($p \leq 0.05$).

Chapter 4

Discussion

4. Discussion

We report a novel interaction mechanism between *P. xylostella* and its host plant, *A. thaliana*. We observed 1. herbivory-responsive miRNAs in *A. thaliana,* which induced as early as 1 h after herbivory; 2. *ath*-miR164 ingestion associated decrease in its putative insect-target transcript, *GSS1*; 3. the hampering of glucosinolate metabolism in larvae, and reduced larval performance upon the *GSS1* targeting *ath*-miR164 ingestion; and 4. a consequent negative effect on the *P. xylostella*'s parasitoid *D. semiclausum*.

Plant miRNA compatibility with insect RNAi components

As a preliminary study, we tested uptake of miRNA forms, and their effects on first instar larvae. A conserved miRNA with a function in regulating developmental timing allowed us to quantify ingested let-7-associated phenotype in the ingesting larvae. We found that miRNA ingestion increased larval endogenous let-7 and pre-let-7 concentrations and reduced two target transcript levels- *FTZ-F1* and *E74*. We observed a distinct let-7-specific response in larvae with a decreased instar duration and larval mass and increased mortality (Liu et al., 2007). Upregulation of *Dicer-1* upon pre-let-7 ingestion suggests the possible role of the miRNA pathway *Dicer* in processing the pre-miRNA. This is also observed in the second-fourth larval instars (Bardapurkar & Pandit, 2023). Interestingly, viral infections have previously been reported to induce Dicers: Dicer in mammalian cells (Poirier et al., 2021) and Dicer-2 in fungi (Aulia et al., 2020), suggesting that Dicers are transcriptionally responsive to foreign RNA. This shows a conserved property of Dicer induction upon foreign ds- or hairpin RNA entry.

After entering the recipient organism, the compatibility of plant miRNAs with the insect RNAi components, especially AGO and Dicer, is crucial. Insect Dicer-1 involved in the miRNA biogenesis shows the absence of the 'DECH' motif in the N-terminal DEAD-like helicase domain, a unique feature of insect Dicer-1 (Tsutsumi et al., 2010). XP_037972432.1, the putative *Pxy*-Dicer-1 showed high structural similarity between both reading domains of *A. thaliana* DCL-1 and *P. xylostella* Dicer-1. This is in parallel to the conserved positively charged insertion in the PAZ N-terminal region between lepidopteran Dicer-1 and plant DCL1 (Arraes et al., 2021), which further supports the similar function of these Dicers.

For plant pre-miRNAs to be processed by the *P. xylostella* dicer, their stem and loop lengths would be comparable to the range of *P. xylostella* pre-miRNAs. Comparative analysis of plant and *insect* pre-miRNAs showed longer stems in plant miRNAs (with

>98% overlap in range), but loop sizes were comparable. This suggests that *Pxy*-Dicer-1 might efficiently process plant (*A. thaliana*) pre-miRNAs with features compatible with *P. xylostella*'s. *ath*-miR164's pre-form is 102 bases, the average length of *P. xylostella* miRNAs, and hence with comparable features.

As average *A. thaliana* pre-miRNA lengths were longer than insects', *Pxy*-Dicer-1 may not efficiently process such longer pre-miRNAs (JE et al., 2011). If true, this poses a selection on the range of pre-miRNAs functioning in the insects. miRNA compatibility with the insect RNAi machinery could be a limiting factor in the evolution of plant miRNA function in insects.

Several studies have elucidated the selection and loading mechanisms of the mature miRNA strand onto AGOs. In *D. melanogaster,* miRNA guide and passenger strands preferentially load on AGO-1 and AGO-2 based on three different features: 5'-end nucleotide, the relative thermodynamic stability of the ends, and the thermodynamic stability of the central region (8-11 nucleotides)(Ghildiyal et al., 2010). However, exceptions exist (Miyoshi et al., 2005, Czech et al., 2009). Our analysis showed that the critical central and terminal bases of *ath*-miRNAs correlate with *Dme*-AGO-1 binding miRNAs more strongly than *Dme*-AGO-2 binding miRNAs. AGO strand selection is known to depend on the physiological conditions in humans, suggesting that selection can be context-dependent (Medley et al., 2021). Experimental validations with AGO-pull down followed by sRNA sequencing will provide strong evidence for AGO selection. Ath-miR164 showed *dme*-AGO-1-binding miRNA-like features with a 5' Uracil and a central mismatch. *Pxy*-Dicer-1 induction in pre-let-7 ingested larvae and miRNA duplex-based feature compatibility with AGO-1 suggest the vital role of the miRNA pathway in processing exogenous miRNAs (Doench et al., 2003). Overall, this *in silico* analysis sheds light on the similarities and differences between plant-insect miRNAs' and the sRNA pathway components' structure and function.

Implications of plant miRNA induction

The plant miRNAs' cross-kingdom action requires miRNA production, followed by stable transfer in the herbivore. Hence, we first studied the response of CP miRNAs to *P. xylostella* herbivory. We identified 13 *A. thaliana* miRNAs induced after *P. xylostella* herbivory, similar to previous miRNA induction studies (Jeyaraj et al., 2017, Wu et al., 2017). This parallels plant-origin secondary metabolites induced in plants only after perceived herbivory (Snoeck et al., 2022). Although induction patterns were miRNA-

specific, most were induced within an hour after larval feeding. This suggests that sRNAs' roles are specified early in plant defense induction. We solely analyzed predicted *P. xylostella* transcript-targeting and excluded all others without predicted targets. One can speculate that several more miRNAs could be herbivory-responsive. A transcriptome-level study identifying time-dependent miRNAs after herbivory could shed more light on the plant's herbivory-responsive miRNome. Several miRNAs' roles in regulating plant transcriptomes in response to insect attacks are known (Ali et al., 2020, Han et al., 2022, Jacob et al., 2021, Kuo et al., 2019, Malhotra et al., 2022). Interestingly, *ath*-miR164 regulates shoot development by regulating the NAC transcription factors, *CUC1* and *CUC2, in planta* (Fang et al., 2014, Rosas Cardenas et al., 2017). Although yet unknown for *CUC1* and *CUC2*, NAC2, an NAC transcription factor is known to balance the growth-defense trade-off in *Capsicum annuum* (Cai et al., 2021). Given their developmental roles, future work could explore the miR164-mediated effects in insect herbivory and plant development in parallel.

The ability of plant miRNAs to target insect transcripts, leading to phenotypic change in the recipient insect, depends on the stable miRNA concentration ingested and present in the insect tissue. The median half-life of the 40 most abundant human miRNAs is 11.4 h, 4 times more than mRNAs (Zlotorynski, 2019). Although *ath*-miR164 production was observed even after 3 days after herbivory, to elucidate if natural *ath*-miR164 levels show *GSS1*-mediated effects in *P. xylostella*, future studies with miRNA mutants, such as overexpression and silenced *ath*-miR164 lines, can be used along with WT. Assessing the role of natural *ath*-miR164 levels on larval *GSS1* levels and, subsequently, the effect on larval performance and natural enemy performance will unfold the ecological implications of the miRNA-mediated cross-kingdom action of miRNAs.

Physiological effects of cross-kingdom miRNA function in P. xylostella

ath-miR164 downregulates *PxGSS1* and *PxGSS2* after 24 h of continuous feeding. This work suggests that along with toxic glucosinolate derivatives as defense molecules, *A. thaliana* has another layer to counter *P. xylostella*'s counter-defense system. We observed reduced larval mass, increased first instar duration, and mortality in miRNA-fed larvae. As expected, this was only true for miRNAs complemented on WT, not the aliphatic glucosinolate-deplete mutant. The absence of glucosinolates nulled the *ath*-miR164-mediated *GSS1*'s effect on larval performance. Apart from *ath*-miR164; *ath*-miR824, and *ath*-miR447 also downregulate *GSS1*. It is thus possible that *A. thaliana* possesses a range

of miRNAs that can regulate the detoxification ability of *P. xylostella*. Zhang et al. showed two *A. thaliana* miRNAs that could potentially modulate the *BJHSP1* and *PPO2* transcripts that regulate pupal development (Zhang et al., 2019). They used injected miRNA mimics to study target downregulation; hence, whether dietary uptake of the miRNAs can regulate insect gene expression remained a question. *PPO2* is an immune system protein involved in melanization and wound healing (Wang et al., 2020), suggesting the involvement of plant miRNAs regulating insects' ability to defend from bacterial infections. Apart from *GSS-1* as a counter-defense transcript, we also observed Cytochrome P450s and carboxypeptidases as other mRNA targets, both protein classes involved in detoxification (Després et al., 2007). Together, Zhang et al. and this study show plant miRNA function in *P. xylostella* hemolymph and gut, respectively. Overall, plant miRNAs could affect gene regulation in many larval tissues, altering larval fitness in a complex manner.

Several other studies have shown the presence of plant miRNAs in larval tissues and predicted their insect mRNA targets (Han et al., 2022, Wang et al., 2017), which in the future can be tested for physiological and ecological relevance.

Multi-trophic effects of cross-kingdom miRNA function

The effect of *ath*-miR164's hampered detoxification response on *P. xylostella* was shown to impact the *D. semiclausum* growth. The wasps' larvae could not persist in a highly toxic environment of the *ath*-miR164-fed *P. xylostella* larvae (Sun et al., 2020), suggesting that miRNA-mediated effects can impact multiple trophic levels. In parallel to the bottom-up miRNA function, *Cotesia vestalis* and its associated virus that parasitizes *P. xylostella* produce miRNAs that can regulate the *P. xylostella* ecdysone receptor (Wang et al., 2018b). This suggests that *P. xylostella* is a hub where multiple organisms at different trophic levels have evolved to use *P. xylostella*'s RNAi machinery to regulate its metabolism.

Conclusion

This study is a classic example of the constant 'tug-of-war' between plants and insects (Snoeck et al., 2022). *A. thaliana* possesses the mustard oil bomb (layer 1) against herbivores such as *P. xylostella*; the larvae possess glucosinolate sulfatase (layer 2) against the eminent plant toxins; and finally, plants possess miRNAs such as *ath*-miR164

(layer 3) that reduce the production of the detoxification proteins. Plants possibly evolved two miRNA functions: *in planta* and *ex planta*.

Future work that details the function of other *GSS* targeting miRNAs, or miRNAs regulating other targets, and their physiological and ecological relevance will construct a detailed picture of the extent of plant miRNAs' role in the *A. thaliana-P. xylostella* interaction. Moreover, this work opens broader questions on the mechanisms of ecological interactions. 1. How ubiquitous is this phenomenon across plant-insect pairs? 2. Does it differ between generalist and specialist insects due to differences in feeding guilds? 4. What portion of the plant miRNA repertoire has insect gene regulatory functions? 5. Can insects counter-defend from plant miRNAs by recognizing these miRNAs? These questions would also contribute to plant miRNAs' increasingly significant role in regulating insect pests.

5. References

Ali, M., Javaid, A., Naqvi, S.H., Batcho, A., Kayani, W.K., Lal, A., Sajid, I.A. and Nwogwugwu, J.O. (2020) Biotic stress triggered small RNA and RNAi defense response in plants. *Molecular Biology Reports,* **47**, 5511-5522.

Arraes, F.B.M., Martins-De-Sa, D., Noriega Vasquez, D.D., Melo, B.P., Faheem, M., De Macedo, L.L.P., Morgante, C.V., Barbosa, J.A.R.G., Togawa, R.C., Moreira, V.J.V., Danchin, E.G.J. and Grossi-De-Sa, M.F. (2021) Dissecting protein domain variability in the core RNA interference machinery of five insect orders. *RNA Biology,* **18**, 1653-1681.

Ashburner, M., Ball, C.A., Blake, J.A., Botstein, D., Butler, H., Cherry, J.M., Davis, A.P., Dolinski, K., Dwight, S.S. and Eppig, J.T. (2000) Gene ontology: tool for the unification of biology. *Nature genetics,* **25**, 25-29.

Aulia, A., Tabara, M., Telengech, P., Fukuhara, T. and Suzuki, N. (2020) Dicer monitoring in a model filamentous fungus host, *Cryphonectria parasitica*. *Current Research in Virological Science,* **1**, 100001.

Bajczyk, M., Jarmolowski, A., Jozwiak, M., Pacak, A., Pietrykowska, H., Sierocka, I., Swida-Barteczka, A., Szewc, L. and Szweykowska-Kulinska, Z. (2023) Recent Insights into Plant miRNA Biogenesis: Multiple Layers of miRNA Level Regulation. *Plants,* **12**, 342-342.

Bally, J., Fishilevich, E., Doran, R.L., Lee, K., De Campos, S.B., German, M.A., Narva, K.E. and Waterhouse, P.M. (2020) Plin-amiR, a pre-microRNA-based technology for controlling herbivorous insect pests. *Plant Biotechnology Journal,* **18**, 1925-1932.

Bardapurkar, R. and Pandit, S. (2023) Trophic microRNA: Precursor and mature microRNA ingestion downregulates the target transcripts and hampers larval development in *Plutella xylostella*. *bioRxiv*, 2023-12.

Benevenuto, R.F., Seldal, T., Hegland, S.J., Rodriguez-Saona, C., Kawash, J. and Polashock, J. (2019) Transcriptional profiling of methyl jasmonate-induced defense responses in bilberry (*Vaccinium myrtillus* L.). *BMC Plant Biology,* **19**.

Bernhart, S.H., Tafer, H., Mückstein, U., Flamm, C., Stadler, P.F. and Hofacker, I.L. (2006) Partition function and base pairing probabilities of RNA heterodimers. *Algorithms for Molecular Biology,* **1**, 1-10.

Bodenhausen, N. and Reymond, P. (2007) Signaling pathways controlling induced resistance to insect herbivores in Arabidopsis. *Molecular Plant-Microbe Interactions,* **20**, 1406-1420.

Boter, M., Ruíz-Rivero, O., Abdeen, A. and Prat, S. (2004) Conserved MYC transcription factors play a key role in jasmonate signaling both in tomato and Arabidopsis. *Genes & development,* **18**, 1577-1591.

Bozorov, T.A., Baldwin, I.T. and Kim, S.-G. (2012) Identification and profiling of miRNAs during herbivory reveals jasmonate-dependent and-independent patterns of accumulation in *Nicotiana attenuata*.

Cai, W., Yang, S., Wu, R., Cao, J., Shen, L., Guan, D. and Shuilin, H. (2021) Pepper NAC-type transcription factor NAC2c balances the trade-off between growth and defense responses. *Plant physiology,* **186**, 2169-2189.

Carthew, R.W. and Sontheimer, E.J. (2009) Origins and Mechanisms of miRNAs and siRNAs. *Cell,* **136**, 642-642.

Chen, C., Ridzon, D.A., Broomer, A.J., Zhou, Z., Lee, D.H., Nguyen, J.T., Barbisin, M., Xu, N.L., Mahuvakar, V.R. and Andersen, M.R. (2005) Real-time quantification of microRNAs by stem–loop RT–PCR. *Nucleic acids research,* **33**, e179-e179.

Chen, W., Dong, Y., Saqib, H.S.A., Vasseur, L., Zhou, W., Zheng, L., Lai, Y., Ma, X., Lin, L., Xu, X., Bai, J., He, W. and You, M. (2020) Functions of duplicated glucosinolate sulfatases in the development and host adaptation of Plutella xylostella. *Insect biochemistry and molecular biology,* **119**.

Choi, W.G., Miller, G., Wallace, I., Harper, J., Mittler, R. and Gilroy, S. (2017) Orchestrating rapid long-distance signaling in plants with Ca2+ , ROS and electrical signals. *The Plant journal : for cell and molecular biology,* **90**, 698-707.

Czech, B., Zhou, R., Erlich, Y., Brennecke, J., Binari, R., Villalta, C., Gordon, A., Perrimon, N. and Hannon, G.J. (2009) Hierarchical Rules for Argonaute Loading in Drosophila. *Molecular Cell,* **36**, 445-456.

De Castro, E., Sigrist, C.J.A., Gattiker, A., Bulliard, V., Langendijk-Genevaux, P.S., Gasteiger, E., Bairoch, A. and Hulo, N. (2006) ScanProsite: Detection of PROSITE signature matches and ProRule-associated functional and structural residues in proteins. *Nucleic Acids Research,* **34**.

Dereeper, A., Guignon, V., Blanc, G., Audic, S., Buffet, S., Chevenet, F., Dufayard, J.F., Guindon, S., Lefort, V., Lescot, M., Claverie, J.M. and Gascuel, O. (2008) Phylogeny.fr: robust phylogenetic analysis for the non-specialist. *Nucleic acids research,* **36**.

Després, L., David, J.P. and Gallet, C. (2007) The evolutionary ecology of insect resistance to plant chemicals. *Trends in ecology & evolution,* **22**, 298-307.

Dexheimer, P.J. and Cochella, L. (2020) MicroRNAs: From Mechanism to Organism. *Frontiers in Cell and Developmental Biology,* **8**, 409-409.

Doench, J.G., Petersen, C.P. and Sharp, P.A. (2003) siRNAs can function as miRNAs. *Genes & Development,* **17**, 438-442.

Donzé, O. and Picard, D. (2002) RNA interference in mammalian cells using siRNAs synthesized with T7 RNA polymerase. *Nucleic acids research,* **30**, e46-e46.

Drerup, M.M., Schlücking, K., Hashimoto, K., Manishankar, P., Steinhorst, L., Kuchitsu, K. and Kudla, J. (2013) The calcineurin B-like calcium sensors CBL1 and CBL9 together with their interacting protein kinase CIPK26 regulate the Arabidopsis NADPH oxidase RBOHF. *Molecular plant,* **6**, 559-569.

Enright, A.J., John, B., Gaul, U., Tuschl, T., Sander, C. and Marks, D.S. (2003) MicroRNA targets in Drosophila. pp. 1-1.

Erb, M. and Reymond, P. (2019) Molecular Interactions Between Plants and Insect Herbivores. *Annual Review of Plant Biology, Vol 70.* (ed. S.S. Merchants), pp. 527-557. Annual Reviews, Palo Alto.

Eswar, N., John, B., Mirkovic, N., Fiser, A., Ilyin, V.A., Pieper, U., Stuart, A.C., Marti-Renom, M.A., Madhusudhan, M.S., Yerkovich, B. and Sali, A. (2003) Tools for comparative protein structure modeling and analysis. *Nucleic Acids Research,* **31**, 3375-3380.

Etebari, K., Afrad, M.H., Tang, B., Silva, R., Furlong, M.J. and Asgari, S. (2018) Involvement of microRNA miR-2b-3p in regulation of metabolic resistance to insecticides in *Plutella xylostella*. *Insect Molecular Biology,* **27**, 478-491.

Etebari, K. and Asgari, S. (2016) Revised annotation of *Plutella xylostella* microRNAs and their genome-wide target identification. *Insect Molecular Biology,* **25**, 788-799.

Fang, Y., Xie, K. and Xiong, L. (2014) Conserved miR164-targeted NAC genes negatively regulate drought resistance in rice. *Journal of experimental botany,* **65**, 2119-2135.

Fathipour, Y. and Mirhosseini, M.A. (2017) Diamondback moth (*Plutella xylostella*) management. *Integrated management of insect pests on canola and other Brassica oilseed crops.* pp. 13-43. CABI Wallingford UK.

Frerigmann, H., Böttcher, C., Baatout, D. and Gigolashvili, T. (2012) Glucosinolates are produced in trichomes of *Arabidopsis thaliana*. *Frontiers in Plant Science,* **3**, 242-242.

Ghildiyal, M., Xu, J., Seitz, H., Weng, Z. and Zamore, P.D. (2010) Sorting of drosophila small silencing RNAs partitions microRNA* strands into the RNA interference pathway. *RNA,* **16**, 43-56.

Giri, A.P., Wunsche, H., Mitra, S., Zavala, J.A., Muck, A., Svatoš, A. and Baldwin, I.T. (2006) Molecular interactions between the specialist herbivore *Manduca sexta* (Lepidoptera, Sphingidae) and its natural host *Nicotiana attenuata*. VII. Changes in the plant's proteome. *Plant Physiology,* **142**, 1621-1641.

Gordon, K.H.J. and Waterhouse, P.M. (2007) RNAi for insect-proof plants. *Nature Biotechnology,* **25**, 1231-1232.

Hammer, D.A.T., Ryan, P.D., Hammer, Ø. and Harper, D.A.T. (2001) Past: Paleontological Statistics Software Package for Education and Data Analysis. *Palaeontologia Electronica.* pp. 178-178.

Han, W.H., Wang, J.X., Zhang, F.B., Liu, Y.X., Wu, H. and Wang, X.W. (2022) Small RNA and Degradome Sequencing Reveal Important MicroRNA Function in Nicotiana tabacum Response to *Bemisia tabaci*. *Genes,* **13**, 361-361.

Handley, R., Ekbom, B. and Ågren, J. (2005) Variation in trichome density and resistance against a specialist insect herbivore in natural populations of *Arabidopsis thaliana*. *Ecological Entomology,* **30**, 284-292.

Iwasaki, S., Kawamata, T. and Tomari, Y. (2009) Drosophila Argonaute1 and Argonaute2 Employ Distinct Mechanisms for Translational Repression. *Molecular Cell,* **34**, 58-67.

Jacob, J., Madhu, P. and Vinodh, R. (2021) Role of miRNA in Plant Defense Against Insects. *Plant-Pest Interactions: From Molecular Mechanisms to Chemical Ecology*, 73-91.

Je, P., I, H., Y, T., Dk, S., H, C., D, J., Dj, P. and Vn, K. (2011) Dicer recognizes the 5' end of RNA for efficient and accurate processing. *Nature,* **475**.

Jeyaraj, A., Liu, S., Zhang, X., Zhang, R., Shangguan, M. and Wei, C. (2017) Genome-wide identification of microRNAs responsive to *Ectropis oblique* feeding in tea plant (*Camellia sinensis* L.). *Scientific Reports,* **7**.

Kawamura, Y., Saito, K., Kin, T., Ono, Y., Asai, K., Sunohara, T., Okada, T.N., Siomi, M.C. and Siomi, H. (2008) Drosophila endogenous small RNAs bind to Argonaute 2 in somatic cells. *Nature 2008 453:7196,* **453**, 793-797.

Kehl, T., Backes, C., Kern, F., Fehlmann, T., Ludwig, N., Meese, E., Lenhof, H.-P. and Keller, A. (2017) About miRNAs, miRNA seeds, target genes and target pathways.

Kelley, L.A., Mezulis, S., Yates, C.M., Wass, M.N. and Sternberg, M.J.E. (2015) The Phyre2 web portal for protein modeling, prediction and analysis. *Nature Protocols,* **10**, 845-858.

Kessler, A. (2015) The information landscape of plant constitutive and induced secondary metabolite production. *Current Opinion in Insect Science.* pp. 47-53. Elsevier Inc.

Kim, Y. and Kim, V.N. (2012) MicroRNA factory: RISC assembly from precursor microRNAs. *Molecular cell,* **46**, 384-386.

Knorr, E., Fishilevich, E., Tenbusch, L., Frey, M.L.F., Rangasamy, M., Billion, A., Worden, S.E., Gandra, P., Arora, K., Lo, W., Schulenberg, G., Valverde-Garcia, P., Vilcinskas, A. and Narva, K.E. (2018) Gene silencing in *Tribolium castaneum* as a tool for the targeted identification of candidate RNAi targets in crop pests. *Scientific Reports 2018 8:1,* **8**, 1-15.

Kozomara, A., Birgaoanu, M. and Griffiths-Jones, S. (2019) MiRBase: From microRNA sequences to function. *Nucleic Acids Research,* **47**, D155-D162.

Krüger, J. and Rehmsmeier, M. (2006) RNAhybrid: MicroRNA target prediction easy, fast and flexible. *Nucleic Acids Research,* **34**.

Kumar, K., Mandal, S.N., Neelam, K. and De Los Reyes, B.G. (2022) MicroRNA-mediated host defense mechanisms against pathogens and herbivores in rice: balancing gains from genetic resistance with trade-offs to productivity potential. *BMC Plant Biology 2022 22:1,* **22**, 1-16.

Kumar, P., Pandit, S.S. and Baldwin, I.T. (2012) Tobacco rattle virus vector: A rapid and transient means of silencing manduca sexta genes by plant mediated RNA interference. *PLoS ONE,* **7**.
Kumar, S., Stecher, G. and Tamura, K. (2016) MEGA7: Molecular Evolutionary Genetics Analysis Version 7.0 for Bigger Datasets. *Molecular Biology and Evolution,* **33**, 1870-1874.
Kuo, Y.W., Lin, J.S., Li, Y.C., Jhu, M.Y., King, Y.C. and Jeng, S.T. (2019) MicroR408 regulates defense response upon wounding in sweet potato. *Journal of Experimental Botany,* **70**, 469-483.
Lee, H., Han, S., Kwon, C.S. and Lee, D. (2016) Biogenesis and regulation of the let-7 miRNAs and their functional implications. *Protein Cell,* **7**, 100-113.
Letunic, I. and Bork, P. (2018) 20 years of the SMART protein domain annotation resource. *Nucleic Acids Research,* **46**, D493-D496.
Li, J.-Y., Chen, Y.-T., Shi, M.-Z., Li, J.-W., Xu, R.-B., Pozsgai, G. and You, M.-S. (2021) Spatio-temporal distribution patterns of *Plutella xylostella* (Lepidoptera: Plutellidae) in a fine-scale agricultural landscape based on geostatistical analysis. *Scientific Reports,* **11**, 13622.
Li, L., Zhu, B., Sun, X., Zheng, K., Liang, P. and Gao, X. (2023) miR-34-5p, a novel molecular target against lepidopteran pests. *Journal of Pest Science,* **96**, 209-224.
Li, X., Guo, L., Zhou, X., Gao, X. and Liang, P. (2015) MiRNAs regulated overexpression of ryanodine receptor is involved in chlorantraniliprole resistance in *Plutella xylostella* (L.). *Scientific Reports,* **5**.
Li, X., Ren, X., Liu, Y., Smagghe, G., Liang, P. and Gao, X. (2020) MiR-189942 regulates fufenozide susceptibility by modulating ecdysone receptor isoform B in *Plutella xylostella* (L.). *Pesticide biochemistry and physiology,* **163**, 235-240.
Liang, P., Feng, B., Zhou, X. and Gao, X. (2013) Identification and developmental profiling of microRNAs in diamondback moth, *Plutella xylostella* (L.). *PLoS One,* **8**.
Ling, L., Ge, X., Li, Z., Zeng, B., Xu, J., Aslam, A.F.M., Song, Q., Shang, P., Huang, Y. and Tan, A. (2014) MicroRNA Let-7 regulates molting and metamorphosis in the silkworm, *Bombyx mori*. *Insect Biochem Mol Biol,* **53**, 13-21.
Liu, S., Xia, Q., Zhao, P., Cheng, T., Hong, K. and Xiang, Z. (2007) Characterization and expression patterns of let-7 microRNA in the silkworm (*Bombyx mori*). *BMC Developmental Biology,* **7**, 1-17.
Lorenz, R., Bernhart, S.H., Höner Zu Siederdissen, C., Tafer, H., Flamm, C., Stadler, P.F. and Hofacker, I.L. (2011) ViennaRNA Package 2.0. *Algorithms for Molecular Biology,* **6**, 1-14.
Lu, S., Wang, J., Chitsaz, F., Derbyshire, M.K., Geer, R.C., Gonzales, N.R., Gwadz, M., Hurwitz, D.I., Marchler, G.H., Song, J.S., Thanki, N., Yamashita, R.A., Yang, M., Zhang, D., Zheng, C., Lanczycki, C.J. and Marchler-Bauer, A. (2020) CDD/SPARCLE: The conserved domain database in 2020. *Nucleic Acids Research,* **48**, D265-D268.
Ma, K., Li, X., Hu, H., Zhou, D., Sun, Y., Ma, L., Zhu, C. and Shen, B. (2017) Pyrethroid-resistance is modulated by miR-92a by targeting CpCPR4 in *Culex pipiens pallens*. *Comparative Biochemistry and Physiology Part B: Biochemistry and Molecular Biology,* **203**, 20-24.
Maffei, M.E., Mithöfer, A. and Boland, W. (2007) Before gene expression: early events in plant-insect interaction. *Trends in Plant Science.* pp. 310-316.
Malhotra, E.V., Jain, R., Tyagi, S., Venkat Raman, K., Bansal, S. and Pattanayak, D. (2022) Identification of dynamic microRNA associated with systemic defence against *Helicoverpa armigera* infestation in *Cajanus scarabaeoides*. *Pest Management Science,* **78**, 3144-3154.
Mamta, B. and Rajam, M.V. (2017) RNAi technology: a new platform for crop pest control. *Physiology and Molecular Biology of Plants,* **23**, 487-501.

Mao, Y.-B., Cai, W.-J., Wang, J.-W., Hong, G.-J., Tao, X.-Y., Wang, L.-J., Huang, Y.-P. and Chen, X.-Y. (2007) Silencing a cotton bollworm P450 monooxygenase gene by plant-mediated RNAi impairs larval tolerance of gossypol. *Nature biotechnology,* **25**, 1307-1313.
Medley, J.C., Panzade, G. and Zinovyeva, A.Y. (2021) microRNA strand selection: Unwinding the rules. *Wiley Interdisciplinary Reviews: RNA,* **12**, e1627.
Mei, Y., Jing, D., Tang, S., Chen, X., Chen, H., Duanmu, H., Cong, Y., Chen, M., Ye, X., Zhou, H., He, K. and Li, F. (2022) InsectBase 2.0: a comprehensive gene resource for insects. *Nucleic Acids Research,* **50**, D1040-D1045.
Min, K. and Lee, J. (2007) RNA interference in C. elegans:History, application, and perspectives. *Integrative Biosciences,* **11**, 99-104.
Miranda, K.C., Huynh, T., Tay, Y., Ang, Y.S., Tam, W.L., Thomson, A.M., Lim, B. and Rigoutsos, I. (2006) A Pattern-Based Method for the Identification of MicroRNA Binding Sites and Their Corresponding Heteroduplexes. *Cell,* **126**, 1203-1217.
Miyoshi, K., Tsukumo, H., Nagami, T., Siomi, H. and Siomi, M.C. (2005) Slicer function of Drosophila Argonautes and its involvement in RISC formation. *Genes & Development,* **19**, 2837-2848.
Morin, M.D., Lyons, P.J., Crapoulet, N., Boquel, S. and Morin, P., Jr. (2017) Identification of differentially expressed miRNAs in Colorado potato beetles (*Leptinotarsa decemlineata* (Say)) exposed to imidacloprid. *International journal of molecular sciences,* **18**, 2728.
Mukherjee, K., Campos, H. and Kolaczkowski, B. (2013) Evolution of animal and plant dicers: Early parallel duplications and recurrent adaptation of antiviral RNA binding in plants. *Molecular Biology and Evolution,* **30**, 627-641.
Mur, L.A.J., Prats, E., Pierre, S., Hall, M.A. and Hebelstrup, K.H. (2013) Integrating nitric oxide into salicylic acid and jasmonic acid/ethylene plant defense pathways. *Frontiers in Plant Science,* **4**, 215-215.
O'brien, J., Hayder, H., Zayed, Y. and Peng, C. (2018) Overview of microRNA biogenesis, mechanisms of actions, and circulation. *Frontiers in Endocrinology,* **9**, 402-402.
Obbard, D.J., Jiggins, F.M., Halligan, D.L. and Little, T.J. (2006) Natural selection drives extremely rapid evolution in antiviral RNAi genes. *Current Biology,* **16**, 580-585.
Pandey, S.P., Shahi, P., Gase, K. and Baldwin, I.T. (2008) Herbivory-induced changes in the small-RNA transcriptome and phytohormone signaling in *Nicotiana attenuata.*
Paturi, S. and Deshmukh, M.V. (2021) A Glimpse of “Dicer Biology” Through the Structural and Functional Perspective. *Frontiers in Molecular Biosciences.* Frontiers Media S.A.
Pettersen, E.F., Goddard, T.D., Huang, C.C., Couch, G.S., Greenblatt, D.M., Meng, E.C. and Ferrin, T.E. (2004) UCSF Chimera - A visualization system for exploratory research and analysis. *Journal of Computational Chemistry,* **25**, 1605-1612.
Poirier, E.Z., Buck, M.D., Chakravarty, P., Carvalho, J., Frederico, B., Cardoso, A., Healy, L., Ulferts, R., Beale, R. and Reis E Sousa, C. (2021) An isoform of Dicer protects mammalian stem cells against multiple RNA viruses. *Science,* **373**, 231-236.
Pratt, A.J. and Macrae, I.J. (2009) The RNA-induced Silencing Complex: A Versatile Gene-silencing Machine. *The Journal of Biological Chemistry,* **284**, 17897-17897.
Pérez-Alonso, M.-M., Sánchez-Parra, B., Ortiz-García, P., Santamaría, M.E., Díaz, I. and Pollmann, S. (2021) Jasmonic Acid-Dependent MYC Transcription Factors Bind to a Tandem G-Box Motif in the YUCCA8 and YUCCA9 Promoters to Regulate Biotic Stress Responses. *International journal of molecular sciences* 22, **22**, 9768.

Rabuma, T., Gupta, O.P. and Chhokar, V. (2022) Recent advances and potential applications of cross-kingdom movement of miRNAs in modulating plant's disease response. *RNA biology*, **19**, 519-532.
Ražná, K. and Cagáň, L.U. (2019) The Role of MicroRNAs in Genome Response to Plant–Lepidoptera Interaction. *Plants,* **8**.
Rosas Cardenas, F.D.F., Ruiz Suárez, Y., Cano Rangel, R.M., Luna Garcia, V., González Aguilera, K.L., Marsch Martínez, N. and De Folter, S. (2017) Effect of constitutive miR164 expression on plant morphology and fruit development in Arabidopsis and tomato. *Agronomy,* **7**, 48.
Roush, S. and Slack, F.J. (2008) The let-7 family of microRNAs. *Trend Cell Biol,* **18**, 505-516.
Saini, R.P., Raman, V., Dhandapani, G., Malhotra, E.V., Sreevathsa, R., Kumar, P.A., Sharma, T.R. and Pattanayak, D. (2018) Silencing of HaAce1 gene by host-delivered artificial microRNA disrupts growth and development of *Helicoverpa armigera*. *PLoS One,* **13**, e0194150.
Sattar, S., Song, Y., Anstead, J.A., Sunkar, R. and Thompson, G.A. (2012) *Cucumis melo* MicroRNA Expression Profile During Aphid Herbivory in a Resistant and Susceptible Interaction. */ 839 MPMI,* **25**, 839-848.
Schmelz, E.A. (2015) Impacts of insect oral secretions on defoliation-induced plant defense. *Current Opinion in Insect Science.* pp. 7-15.
Scholz, S.S., Vadassery, J., Heyer, M., Reichelt, M., Bender, K.W., Snedden, W.A., Boland, W. and Mithöfer, A. (2014) Mutation of the Arabidopsis calmodulin-like protein CML37 deregulates the jasmonate pathway and enhances susceptibility to herbivory. *Molecular plant,* **7**, 1712-1726.
Schuman, M.C. and Baldwin, I.T. (2016) The Layers of Plant Responses to Insect Herbivores. *Annual Review of Entomology.* pp. 373-394. Annual Reviews Inc.
Shelton, A.M., Cooley, R.J., Kroening, M.K., Wilsey, W.T. and Eigenbrode, S.D. (1991) Comparative analysis of two rearing procedures for diamondback moth (Lepidoptera: Plutellidae). *J Entomol Sci,* **26**, 17-26.
Snoeck, S., Guayazán-Palacios, N. and Steinbrenner, A.D. (2022) Molecular tug-of-war: Plant immune recognition of herbivory. *The Plant Cell,* **34**, 1497-1513.
Song, J. and Zhou, S. (2020) Post-transcriptional regulation of insect metamorphosis and oogenesis. *Cell Mol Life Sci,* **77**, 1893-1909.
Sun, R., Gols, R., Harvey, J.A., Reichelt, M., Gershenzon, J., Pandit, S.S. and Vassão, D.G. (2020) Detoxification of plant defensive glucosinolates by an herbivorous caterpillar is beneficial to its endoparasitic wasp. *Molecular Ecology,* **29**, 4014-4031.
Sun, R., Jiang, X., Reichelt, M., Gershenzon, J., Pandit, S.S. and Giddings Vassão, D. (2019) Tritrophic metabolism of plant chemical defenses and its effects on herbivore and predator performance. *Elife,* **8**, e51029.
Sønderby, I.E., Hansen, B.G., Bjarnholt, N., Ticconi, C., Halkier, B.A. and Kliebenstein, D.J. (2007) A Systems Biology Approach Identifies a R2R3 MYB Gene Subfamily with Distinct and Overlapping Functions in Regulation of Aliphatic Glucosinolates. *PLOS ONE,* **2**, e1322-e1322.
Tang, W., Yu, L., He, W., Yang, G., Ke, F., Baxter, S.W., You, S., Douglas, C.J. and You, M. (2014) DBM-DB: The diamondback moth genome database. *Database,* **2014**.
Thomas, P.D., Ebert, D., Muruganujan, A., Mushayahama, T., Albou, L.P. and Mi, H. (2022) PANTHER: Making genome-scale phylogenetics accessible to all. *Protein Science,* **31**, 8-22.
Thompson, J.D., Higgins, D.G. and Gibson, T.J. (1994) CLUSTAL W: improving the sensitivity of progressive multiple sequence alignment through sequence weighting, position-specific gap penalties and weight matrix choice. *Nucleic acids research,* **22**, 4673-4680.

Timmons, L., Court, D.L. and Fire, A. (2001) Ingestion of bacterially expressed dsRNAs can produce specific and potent genetic interference in *Caenorhabditis elegans*. *Gene,* **263**, 103-112.
Tomoyasu, Y., Miller, S.C., Tomita, S., Schoppmeier, M., Grossmann, D. and Bucher, G. (2008) Exploring systemic RNA interference in insects: a genome-wide survey for RNAi genes in Tribolium. *Genome biology,* **9**, 1-22.
Toyota, M., Spencer, D., Sawai-Toyota, S., Jiaqi, W., Zhang, T., Koo, A.J., Howe, G.A. and Gilroy, S. (2018) Glutamate triggers long-distance, calcium-based plant defense signaling. *Science,* **361**, 1112-1115.
Tsutsumi, A., Kawamata, T., Izumi, N., Seitz, H. and Tomari, Y. (2010) Recognition of the pre-miRNA structure by Drosophila-Dicer-1. *Nature Structural and Molecular Biology,* **18**, 1153-1158.
Vogel, E., Santos, D., Mingels, L., Verdonckt, T.-W. and Broeck, J.V. (2019) RNA interference in insects: protecting beneficials and controlling pests. *Frontiers in physiology,* **9**, 1912.
Vorozheykin, P.S. and Titov, I.I. (2020) Erratum to: How Animal miRNAs Structure Influences Their Biogenesis (Russian Journal of Genetics, (2020), 56, 1, (17-29), 10.1134/S1022795420010135). *Russian Journal of Genetics.* pp. 1012-1024. Pleiades Publishing.
Wang, H., Zhang, C., Dou, Y., Yu, B., Liu, Y., Heng-Moss, T.M., Lu, G., Wachholtz, M., Bradshaw, J.D., Twigg, P., Scully, E., Palmer, N. and Sarath, G. (2017) Insect and plant-derived miRNAs in greenbug (*Schizaphis graminum*) and yellow sugarcane aphid (Sipha flava) revealed by deep sequencing. *Gene,* **599**, 68-77.
Wang, J., Mei, J. and Ren, G. (2019a) Plant microRNAs: Biogenesis, homeostasis, and degradation. *Frontiers in Plant Science,* **10**, 360-360.
Wang, J.J., Wu, D.W., Wang, Y.P. and Xie, D.X. (2019b) Jasmonate action in plant defense against insects. *Journal of Experimental Botany,* **70**, 3391-3400.
Wang, K., Su, X., Cui, X., Du, Y., Zhang, S. and Gao, J. (2018a) Identification and Characterization of microRNA during Bemisia tabaci Infestations in Solanum lycopersicum and *Solanum habrochaites*. *Horticultural Plant Journal,* **4**, 62-72.
Wang, N.-M., Li, J.-J., Shang, Z.-Y., Yu, Q.-T. and Xue, C.-B. (2020) Increased responses of phenoloxidase in chlorantraniliprole resistance of *Plutella xylostella* (Lepidoptera: Plutellidae). *Journal of Insect Science,* **20**, 2.
Wang, Z.-Z., Ye, X.-Q., Shi, M., Li, F., Wang, Z.-H., Zhou, Y.-N., Gu, Q.-J., Wu, X.-T., Yin, C.-L. and Guo, D.-H. (2018b) Parasitic insect-derived miRNAs modulate host development. *Nature Communications,* **9**, 2205.
Waterhouse, A., Bertoni, M., Bienert, S., Studer, G., Tauriello, G., Gumienny, R., Heer, F.T., De Beer, T.A.P., Rempfer, C., Bordoli, L., Lepore, R. and Schwede, T. (2018) SWISS-MODEL: Homology modelling of protein structures and complexes. *Nucleic Acids Research,* **46**, W296-W303.
Wei, X., Zheng, C., Peng, T., Pan, Y., Xi, J., Chen, X., Zhang, J., Yang, S., Gao, X. and Shang, Q. (2016) miR-276 and miR-3016-modulated expression of acetyl-CoA carboxylase accounts for spirotetramat resistance in *Aphis gossypii* Glover. *Insect biochemistry and molecular biology,* **79**, 57-65.
Wu, Y., Lv, W., Hu, L., Rao, W., Zeng, Y., Zhu, L., He, Y. and He, G. (2017) Identification and analysis of brown planthopper-responsive microRNAs in resistant and susceptible rice plants. *Scientific Reports,* **7**.
Xia, X., Shao, Y., Jiang, J., Du, X., Sheng, L., Chen, F., Fang, W., Guan, Z. and Chen, S. (2015) MicroRNA expression profile during aphid feeding in chrysanthemum (*Chrysanthemum morifolium*). *PLoS ONE,* **10**.
Yu, X., Zhou, Q., Li, S.-C., Luo, Q., Cai, Y., Lin, W.-C., Chen, H., Yang, Y., Hu, S. and Yu, J. (2008) The silkworm (*Bombyx mori*) microRNAs and their expressions in multiple developmental stages. *PloS one,* **3**, e2997.
Zafar, J., Zhang, Y., Huang, J., Freed, S., Shoukat, R.F., Xu, X. and Jin, F. (2021) Spatio-temporal profiling of Metarhizium anisopliae—responsive microRNAs

involved in modulation of *Plutella xylostella* immunity and development. *Journal of Fungi,* **7**, 942.
Zalucki, M.P., Shabbir, A., Silva, R., Adamson, D., Liu, S.S. and Furlong, M.J. (2012) Estimating the economic cost of one of the world's major insect pests, *Plutella xylostella* (Lepidoptera: Plutellidae): just how long is a piece of string? *Journal of economic entomology,* **105**, 1115-1129.
Zardoya, R. (2021) Quest for the best evolutionary model. *Journal of Molecular Evolution,* **89**, 146-150.
Zebelo, S.A. and Maffei, M.E. (2015) Role of early signalling events in plant-insect interactions. *Journal of Experimental Botany.* pp. 435-448. Oxford University Press.
Zhang, K., Hodge, J., Chatterjee, A., Moon, T.S. and Parker, K.M. (2021) Duplex structure of double-stranded RNA provides stability against hydrolysis relative to single-stranded RNA. *Environmental Science & Technology,* **55**, 8045-8053.
Zhang, L.L., Jing, X.D., Chen, W., Wang, Y., Lin, J.H., Zheng, L., Dong, Y.H., Zhou, L., Li, F.F., Yang, F.Y., Peng, L., Vasseur, L., He, W.Y. and You, M.S. (2019) Host plant-derived miRNAs potentially modulate the development of a cosmopolitan insect pest, *Plutella xylostella*. *Biomolecules,* **9**.
Zhang, R., Jing, Y., Zhang, H., Niu, Y., Liu, C., Wang, J., Zen, K., Zhang, C.Y. and Li, D. (2018) Comprehensive Evolutionary Analysis of the Major RNA-Induced Silencing Complex Members. *Scientific Reports 2018 8:1,* **8**, 1-7.
Zhang, Y.L., Huang, Q.X., Yin, G.H., Lee, S., Jia, R.Z., Liu, Z.X., Yu, N.T., Pennerman, K.K., Chen, X. and Guo, A.P. (2015) Identification of microRNAs by small RNA deep sequencing for synthetic microRNA mimics to control *Spodoptera exigua*. *Gene,* **557**, 215-221.
Zhu, B., Li, X., Liu, Y., Gao, X. and Liang, P. (2017) Global identification of microRNAs associated with chlorantraniliprole resistance in diamondback moth *Plutella xylostella* (L.). *Scientific Reports,* **7**.
Zhu, K.Y. and Palli, S.R. (2020) Mechanisms, applications, and challenges of insect RNA interference. *Annual review of entomology,* **65**, 293-311.
Zlotorynski, E. (2019) Insights into the kinetics of microRNA biogenesis and turnover. *Nature Reviews Molecular Cell Biology,* **20**, 511-511.
Zotti, M.J. and Smagghe, G. (2015) RNAi technology for insect management and protection of beneficial insects from diseases: lessons, challenges and risk assessments. *Neotropical Entomology,* **44**, 197-213.